To the Graduate Council:

I am submitting herewith a dissertation written by Izabela Szlufarska entitled "Spin excitations in quantum Hall systems and their effect on nuclear spin relaxation and photoluminescence". I have examined the final paper copy of this dissertation for form and content and recommend that it be accepted in partial fulfillment of the requirements for the degree of Doctor of Philosophy, with a major in Physics.

John J. Quinn, Major Professor

We have read this dissertation
and recommend its acceptance:

Accepted for the Council:

Vice Provost and Dean of
Graduate Studies

SPIN EXCITATIONS IN QUANTUM HALL SYSTEMS AND THEIR EFFECT ON NUCLEAR SPIN RELAXATION AND PHOTOLUMINESCENCE

A Dissertation

Presented for the

Doctor of Philosophy

Degree

The University of Tennessee, Knoxville

Izabela Szlufarska

May, 2002

Acknowledgement

I am greatly indebted to Prof. John J. Quinn who has been of invaluable help throughout my academic career and during the research for this dissertation. It has been a pleasure to learn from someone who is not only an excellent physicist, but also takes great care of his students and employees. I would also like to sincerely thank Dr. Arkadiusz Wójs who has contributed in an important way to the progress of my work to this point through discussions and help in developing computer programs.

I also wish to express a deep appreciation for the support of my parents, Wacław and Grażyna Szlufarscy, my sister Agnieszka and all my wonderful friends, both in Knoxville and in Poland.

Abstract

Two problems with respect to spin excitations in quantum Hall systems are studied by means of exact numerical diagonalization. The first one is related to the formation of reversed-spin quasielectrons (QE_R) in a two-dimensional electron gas (2DEG). The single-particle properties of QE_R's as well as the pseudopotentials of their interaction with one another and with Laughlin quasielectrons (QE's) and quasiholes (QH's) are calculated. Based on the short-range character of the QE_R–QE_R and QE_R–QE repulsion, the partially unpolarized incompressible states at the filling factors $\nu = \frac{4}{11}$ and $\nu = \frac{5}{13}$ are postulated within Haldane's hierarchy scheme. To describe photoluminescence, the family of bound $h(QE_R)_n$ states of a valence hole h and n QE_R's are predicted in analogy to the found earlier fractionally charged excitons hQE_n. The binding energy and optical selection rules for both families are compared. The hQE_R is found radiative in contrast to the dark hQE, and the $h(QE_R)_2$ is found nonradiative in contrast to the bright hQE_2. The second problem involves the numerical study of the relaxation rates of nuclear spins coupled through the hyperfine interaction to a 2DEG at magnetic fields corresponding to both fractional and integral Landau level fillings ν. The spectral functions $\tau^{-1}(E)$ describing the response of the 2DEG to the reversal of an embedded localized spin are calculated. In a (locally) incompressible $\nu = 1$ or $\frac{1}{3}$ state, the finite Coulomb energy of short spin waves, together with the small nuclear Zeeman energy, prevent nuclear spin relaxation even in the limit of vanishing electron Zeeman energy (E_Z). However, we find that the nuclear spins can couple to the internal excitations of mobile finite-size skyrmions that appear in the 2DEG at sufficiently low E_Z and at ν slightly different from 1 or $\frac{1}{3}$. The experimentally observed dependence of nuclear spin relaxation rate on E_Z and ν is explained in terms of the occurrence of skyrmions and anti-skyrmions of various topological charge.

Contents

1 Overview **1**

2 Quantum Hall Systems **7**

2.1 Integral and Fractional Quantum Hall Effect 7

2.2 Laughlin Wave Function 11

2.3 Composite Fermion Picture 13

2.4 Coulomb Pseudopotential and Composite Fermion Picture 15

2.5 Composite Fermions with a Spin Freedom 17

3 Numerical Studies **19**

3.1 Haldane Sphere 19

3.2 Many-Body States 23

3.3 Mean-Field Composite Fermion Picture in Spherical Geometry 25

4 Energy, Interaction and Photoluminescence of Spin-Reversed Quasielectrons **29**

4.1 Introduction 29

4.2 Stability and Single Particle Properties of Spin-Reversed Quasielectrons 32

4.3 Interaction with Other Quasiparticles 37

4.4 Optical Properties 42

5 Spin Flip Excitations and Skyrmions **47**

6 Hyperfine Coupling of Quantum Hall States to Nuclear Spins **51**

6.1 Introduction 51

6.2 Model 52

6.3 Integral Quantum Hall Regime 56

6.4 Fractional Quantum Hall Regime 61

Bibliography **66**

Vita **79**

List of Figures

2.1 Density of states vs. energy E. 9

2.2 FQHE in the lowest LL at $\nu = \frac{1}{3}$ [108]. ρ_{xy} and ρ_{xx} are the Hall and longitudinal resistivities. 10

4.1 Elementary excitations of the $\nu = \frac{1}{3}$ Laughlin state. (a) The energy spectrum (Coulomb energy E versus angular momentum L) of the system of $N = 9$ electrons on Haldane sphere at the monopole strength $2Q = 3(N-1) = 24$. Black dots and grey diamonds mark states with the total spin $S = \frac{1}{2}N = \frac{9}{2}$ (maximum polarization) and $S = \frac{1}{2}N - 1 = \frac{7}{2}$ (one reversed spin), respectively. Ground state is the Laughlin $\nu = \frac{1}{3}$ state. Lines connect states containing one QE–QH ($S = \frac{9}{2}$) or $\mathrm{QE_R}$–QH ($S = \frac{7}{2}$) pair. (b) The dispersion curves (excitation energy $\mathcal{E}_K = E - E_0$ versus wave vector k) for the $K = 0$ charge-density wave (QE–QH pair) and the $K = 1$ spin-density wave ($\mathrm{QE_R}$–QH pair) in the Laughlin $\nu = \frac{1}{3}$ ground state, calculated in the systems of $N \leq 11$ electrons on Haldane sphere. λ is the magnetic length and K is the number of reversed spins relative to a ferromagnetic state [105] 33

4.2 Quasiparticles in the $\nu = \frac{1}{3}$ Laughlin ground state. (a) The energy spectrum (Coulomb energy E versus angular momentum L) of the system of $N = 9$ electrons on Haldane sphere at the monopole strength $2Q = 3(N-1) - 1 = 23$. Black dots and grey diamonds mark states with the total spin $S = \frac{1}{2}N = \frac{9}{2}$ (maximum polarization) and $S = \frac{1}{2}N - 1 = \frac{7}{2}$ (one reversed spin), respectively. Ground state at $S = \frac{7}{2}$ is the reversed-spin quasielectron $\mathrm{QE_R}$ of the Laughlin $\nu = \frac{1}{3}$ fluid, and the lowest-energy state at $S = \frac{9}{2}$ is the Laughlin quasielectron QE. (b) The energies ε of all three types of quasiparticles of the $\nu = \frac{1}{3}$ state (QH, QE, and $\mathrm{QE_R}$) calculated in the systems of $N \leq 11$ electrons on Haldane sphere and plotted as a function of N^{-1}. The numbers give the results of linear extrapolation to an infinite (planar) system. λ is the magnetic length. [105] 36

4.3 Interaction between two $\mathrm{QE_R}$'s. (a) The energy spectrum (Coulomb energy E versus angular momentum L) of the system of $N = 8$ electrons on Haldane sphere at the monopole strength $2Q = 3(N-1)-2 = 19$. Black dots, grey diamonds, and open circles mark states with the total spin $S = \frac{1}{2}N = 4$ (maximum polarization), $S = \frac{1}{2}N - 1 = 3$ (one reversed spin), and $S = \frac{1}{2}N - 2 = 2$ (two reversed spins), respectively. Lines connect states containing one QE–QE ($S = 4$), QE–$\mathrm{QE_R}$ ($S = 3$), or $\mathrm{QE_R}$–$\mathrm{QE_R}$ ($S = 2$) pair. (b) The pseudopotentials (pair energy V versus relative angular momentum $\mathcal{R}$) of the $\mathrm{QE_R}$–$\mathrm{QE_R}$ interaction calculated in the systems of $N \leq 9$ electrons on Haldane sphere. λ is the magnetic length. [105] 38

4.4 Interaction between QE and $\mathrm{QE_R}$. (a) The energy spectrum (Coulomb energy E versus angular momentum L) of the system of $N = 9$ electrons on Haldane sphere at the monopole strength $2Q = 3(N-1) - 2 = 22$. Black dots and grey diamonds mark states with the total spin $S = \frac{1}{2}N = \frac{9}{2}$ (maximum polarization) and $S = \frac{1}{2}N - 1 = \frac{7}{2}$ (one reversed spin), respectively. Lines connect states containing one QE–QE ($S = \frac{9}{2}$) or QE–$\mathrm{QE_R}$ ($S = \frac{7}{2}$) pair. (b) The pseudopotentials (pair energy V versus relative angular momentum $\mathcal{R}$) of the QE–$\mathrm{QE_R}$ interaction calculated in the systems of $N \leq 10$ electrons on Haldane sphere. λ is the magnetic length. [105] 40

4.5 Interaction between quasiparticles and a valence band hole. (a) The pseudopotentials (pair energy V versus pair angular momentum L) of the h–$\mathrm{QE_R}$ interaction calculated in the system of $N = 7$ electrons and one valence hole (h) on Haldane sphere at the monopole strength $2Q = 3(N-1) - 1 = 17$. Different symbols correspond to different separations d between the electron and hole planes. (bcd) The energy spectra (Coulomb energy E versus angular momentum L) of the same, seven-electron–one-hole system at $2Q = 17$ at three different values of d. Black dots and grey diamonds mark states with the total electron spin $S = \frac{1}{2}N = \frac{7}{2}$ (maximum polarization) and $S = \frac{1}{2}N - 1 = \frac{5}{2}$ (one reversed spin), respectively. Lines in (d) connect states containing one h–QE ($S = \frac{7}{2}$) or h–$\mathrm{QE_R}$ ($S = \frac{5}{2}$) pair. The lowest-energy $S = \frac{7}{2}$ and $\frac{5}{2}$ states in (c) are the fractionally charged excitons, $h\mathrm{QE}$ and $h\mathrm{QE_R}$, respectively. λ is the magnetic length. [105] 43

4.6 The energy spectra (Coulomb energy E versus angular momentum L) of the system of $N = 7$ electrons and one valence hole (h) on Haldane sphere at the monopole strength $2Q = 3(N-1) - 2 = 16$, at the separations $d = 2\lambda$ (a) and 4λ (b) between the electron and hole planes. Black dots, grey diamonds, and open circles mark states with the total electron spin $S = \frac{1}{2}N = \frac{7}{2}$ (maximum polarization), $S = \frac{1}{2}N - 1 = \frac{5}{2}$ (one reversed spin), and $S = \frac{1}{2}N - 2 = \frac{3}{2}$ (two reversed spins), respectively. The lowest-energy $S = \frac{7}{2}$, $\frac{5}{2}$, and $\frac{3}{2}$ states in (a) are the fractionally charged excitons, $h\mathrm{QE}_2$, $h\mathrm{QE_RQE}$, and $h(\mathrm{QE_R})_2$, respectively. The lowest-energy band of $S = \frac{3}{2}$ states marked with lines in (b) contains all possible states of two $\mathrm{QE_R}$'s and one h. λ is the magnetic length. [105] 46

5.1 A finite system of $N = 12$ electrons at $2Q = 12$ ($\nu = 1^{\pm}$). (a) The excitation energy from the ferromagnetic GS E_0 to a skyrmionic state E_S vs the topological charge of the skyrmion K (number of SW's created in a system); open symbols: in the absence of the Zeeman energy; solid dots: adding the Zeeman energy E_Z causes transition to the GS with $K = 3$ (circled). (b) The reduced energy gap between the skyrmionic GS $E_{GS}(K)$ and the first excited state E_{ex} as a function of the Zeeman energy E_Z. The $E = E_Z$ function is the corresponding energy gap at precisely $\nu = 1$. [107] 48

6.1 Transitions from the $\nu = 1$ Laughlin ground state induced by hyperfine interaction with a localized spin. (a) The energy E of transitions vs angular momentum L and wave vector $k\lambda$ for a system of $N = 20$ electrons filling exactly the lowest LL ($2Q = 19$). Bubble size is proportional to τ^{-1}. Solid dots and crosses mark states with $K = 0$ and 1 reversed spins, respectively. (b) The transition probability (normalized by $\sqrt{N}$) as a function of energy E for $N \leq 25$. (c) and (d) The spectral functions $\tau^{-1}(k\lambda)$ and $\tau^{-1}(E)$, respectively, in the planar geometry limit ($N \to \infty$). [107] 56

6.2 The intensity τ^{-1} vs energy E and the energy spectra (insets) of $N = 12$ electrons at $2Q = 12$ ($\nu = 1^{\pm}$) for transitions from initial states: (a) $K = 0, L_z = -5$ (a h next to the nucleus), (b)$K = 1, L_z = -4$ (S_1^+ next to the nucleus) (c)$K = 1, L_z = -2$ (S_1^+ moved away from the nucleus) (d)$K = 1, L_z = -3$ (S_2^+ at the nucleus). The d and u symbols correspond to the $\downarrow$- and $\uparrow$-spin polarization. [107] 59

6.3 Intensities of transitions in the $\nu = 1^{\pm}$ fluid in the limit of $N^{-1} \to 0$. (a) The intensity τ^{-1} vs N^{-1} for transitions from the skyrmion states with $K \leq 4$ (marked with different symbols) to final states with $K \pm 1$ due to the hyperfine interaction with a nucleus. (b) The transition probability τ^{-1} between skyrmionic states $K \to K \pm 1$ vs K in a system of $N = 12$ electrons. (c) The intensity of transitions $K \to K \pm 1$ as a function of the Zeeman energy. K is the number of reversed spins in the initial state; the solid line is a Gaussian expected to be observed in experiment. (d) Same as (b) but in the $N^{-1} \to 0$ limit (planar system). [107] 60

6.4 Transitions from the $\nu = \frac{1}{3}$ ground state. (a) The energy E of transition from the ferromagnetic GS of the system of $N = 6$ electrons at $2Q = 15$ ($\nu = \frac{1}{3}$) as a function of angular momentum L and wave vector $k\lambda$. The final states have $K = 0$ (solid dots) and $K = 1$ (open circles) number of reversed spins, respectively. Bubble size corresponds to the transition intensity τ^{-1}. (b) The transition probability (normalized by $\sqrt{N}$) vs energy E for $N \leq 8$. The spectral functions $\tau^{-1}(k\lambda)$ and $\tau^{-1}(E)$ in the planar system (infinite Haldane sphere) are shown in (c) and (d). [107] 62

6.5 τ^{-1} vs energy E and the energy spectra (insets) of the system of $N = 6$ electrons at $\nu = \frac{1}{3}^{\pm}$ for the transitions from the following initial states: (a) QH in the $n = 0$ spin-$\downarrow$ LL ($2Q = 16$), (b) QE in the first excited spin-$\downarrow$ LL ($2Q = 14$), (c) $\mathrm{QE_R}$ in the $n = 0$ spin-$\uparrow$ LL ($2Q = 14$), (d) skyrmion S_2^+ (two SW's bound to a QH, $2Q = 14$). The d and u symbols correspond to the $\downarrow$- and $\uparrow$-spin polarization. [107] 64

List of Tables

3.1 The dimension N_ϕ of the single particle Landau level, dimension $N_{\rm MB}$ of the total many body Hilbert space, dimension $N_{\rm MB}(0)$ of the largest (M) subspace, dimension $N_{\rm MB}^{\rm MAX}(M,L)$ of the largest (M,L) subspace and dimension $N_{\rm MB}(0,0)$ of the (M,L) subspace containing the Laughlin $L=0$ ground state, of $N=6$ to 11 electrons at the filling factor $\nu=\frac{1}{3}$ [119]. 25

Chapter 1

Overview

The integral quantum Hall (IQH) effect [55] and the fractional quantum Hall (FQH) effect [108] refer to quantization of the Hall conductance of a two-dimensional electron gas (2DEG) in high magnetic fields. Both IQH and FQH effects are a manifestation of the occurrence of finite excitation gaps that open above incompressible non-degenerate ground states (GS's) at certain (integral or fractional, respectively) Landau level (LL) fillings ν. However, while the single-particle energy gap responsible for IQH effect results from transport properties of electrons, the gap separating a FQH incompressible GS from the excited states is due to electron-electron interactions.

The physics of the most prominent FQH states at $\nu = 1/m$ (where m is an odd number) has been explained by Laughlin [62], who proposed a wave function for such incompressible GS's and described their elementary excitations in terms of quasiparticles (QP's): quasielectrons (QE's) and quasiholes (QH's). Laughlin's idea has been later extended by Haldane [36] and others [41, 48, 64, 98], who independently proposed various hierarchy schemes, in which the QP's form Laughlin-like states of their own. The hierarchy theory was shown [56, 72, 92, 108, 112] to have a serious shortcoming: it predicts incompressible states at some simple fractions that do not occur in experiment, whereas explanation of some other, experimentally observed ones involves many levels of hierarchy.

An alternative picture of the FQH states is offered by the mean-field composite fermion (CF) approach, introduced by Jain [47] and developed by Lopez and Fradkin [67] and by Halperin, Lee, and Read [42]. The CF's are constructed in the Chern-Simons (CS) gauge transformation by attaching to each electron a tube carrying an even number of magnetic flux quanta. In the mean-field approximation the CF's move in an effective field B^*, lower than the original field B seen by electrons. It was conjectured that the gas of strongly interacting electrons behaves as a gas of weakly interacting CF's, and that the FQH effect of electrons can be interpreted as the IQH effect of CF's.

The success of the mean-field CF picture in predicting the band of lowest-energy multiplets of FQH systems led to the conjecture that Coulomb and CS gauge interactions beyond the mean-field cancel each other, which assumption cannot possibly be correct because of different energy scales involved [119]. It has been shown [120, 122] that the reason for the success is related to the character of the Coulomb pseudopotential, defined as the dependence of the pair interaction energy V on the pair angular momentum L (or on the relative pair angular momentum $\mathcal{R}$).

Remarkably, the Laughlin $\nu = 1/m$ GS's are the only FQH states that are maximally spin polarized solely due to the electron-electron exchange interaction. At other filling factors, the 2DEG is only partially polarized [3, 14, 17, 40, 127, 128, 134], unless the Zeeman energy E_Z is sufficiently large. It was Rezayi [91] and Chakraborty *et al.* [15] who discovered that in addition to a spatially separated QE–QH pair, another low-energy excitation of the Laughlin state exists, a spin-density wave, consisting of a QH bound to a reversed-spin quasielectron (QE_R). The spin excitations of Laughlin states have been extensively studied in the context of skyrmions [66, 102], however the knowledge of their interaction with one another or with other excitations, or their optical properties is not yet complete.

In the course of this work we address both of these issues, and using exact numerical diagonalization we study the properties of the QE_R's in the FQH regime (at $\nu = \frac{1}{3}$). We calculate the pseudopotentials $V(\mathcal{R})$ describing interaction of QE_R's with one another

and with other Laughlin QP's. From the form of the QE_R–QE_R pseudopotential we show that the Haldane-hierarchy $\nu = \frac{1}{3}$ daughter state of QE_R's formed in the parent $\nu = \frac{1}{3}$ Laughlin state of electrons is incompressible. This state corresponds to the total electron filling factor of $\nu = \frac{4}{11}$ and partial, 75% spin polarization. Because the analogous $\nu = \frac{1}{3}$ hierarchy state of QE's is known to be compressible, we conclude that the experimentally observed [104] FQH effect at $\nu = \frac{4}{11}$ confirms the formation of QE_R's and their Laughlin correlations in a 2DEG with low Zeeman splitting. Although the stability of mixed QE–QE_R hierarchy states is expected to be highly sensitive to the Zeeman energy E_Z, we predict that an incompressible state that corresponds to $\nu = \frac{5}{13}$ and 80% spin polarization may form at appropriate E_Z.

We also study the interaction of QE_R's with a spatially separated valence-band hole. In analogy to the so-called fractionally charged exciton (FCX) states hQE_n, we predict the occurrence of the spin-reversed complexes FCX_R that involve one or more QE_R's. Because QE and QE_R have different angular momenta, the optical selection rules for FCX and FCX_R are different, and, for example, hQE_R turns out radiative in contrast to the dark hQE, while $h(QE_R)_2$ is dark in contrast to the bright hQE_2, Therefore, in addition to obvious difference in polarization, the emission from FCX and FCX_R states is expected to occur at a different energy and differently depend on temperature.

Interestingly, what really causes the abrupt depolarization of a 2DEG in the quantum Hall regime is the insertion of an extra particle (a reversed-spin electron or a hole) to the ferromagnetic GS. It results in the formation of skyrmions [66, 99, 102, 129], well defined particle-like charged spin excitations which move in the underlying incompressible fluid. The criterion that allows prediction and explanations of the occurrence or absence of skyrmions, formulated by Wójs and Quinn [125] is based on the analysis of the involved interaction pseudopotentials.

The interest in magnetic properties of semiconductor heterostructures in high magnetic fields has been significantly increased due to the recent advances in the field of quantum electronics related to spin polarization [5, 10, 110]. The first proposal for quan-

tum computing suggested using as quantum bits (qubits) an array of quantum dots [68] coupled by electron tunneling. Another natural choice for qubits are spin states of nuclei or electrons in semiconductors [26, 45, 52, 88], because of their relatively long life-times at low temperatures (which affect decoherence rates). The first such proposal [88] was based on nuclear spins in heterojunctions [26, 79, 87, 111] coupled by the hyperfine interaction to a 2DEG in the highly correlated and nondissipative integral quantum Hall state [86]. The idea of utilizing these systems for quantum computation was motivated by optically pumped NMR experiments [5, 110] in GaAs heterostructures that showed a dramatic drop of the nuclear relaxation time and a sharp decrease of the Knight shift when the filling factor ν was moved away from the precise value of $\nu = 1$. Similar effects were observed [24] near $\nu = \frac{1}{3}$. It is therefore expected that the quantum information written on nuclear spins can be frozen for a relatively long time (of the order of seconds [26, 79]) when the 2DEG is tuned to $\nu = 1$ or $\frac{1}{3}$, and manipulated by varying ν away from those values.

A detailed review of the work on spin based quantum computing in semiconductor structures can be found in the article of Privman *et al.* [87]. One of the major theoretical tasks is to understand the processes and time scales involved in the dynamics of actual computation. Due to the computational difficulties, the relaxation processes considered in the literature [34, 74, 80, 84, 109] are associated only with few-qubit systems, and the single-qubit times are usually used to describe their dynamics. There have been various attempts to evaluate the relaxation times of the nuclear spins with interactions mediated by 2DEG. A dominant approach, which accounts for the entanglement of the system with the environment and resulting additional couplings, involves the evolution of a density matrix [74]. It is predicted that in order to describe multi-qubit systems, the inclusion of "quantum chaos" effects may be eventually required [8, 9].

The relaxation processes of nuclear spins were observed in experiments where nuclei in a quantum well (QW) were first polarized by optical pumping, and subsequently allowed to relax through the hyperfine interaction with the surrounding 2DEG in the

quantum Hall regime [5, 10, 12, 110]. The change in nuclear polarization (proportional to the Overhauser shift) is measured [12, 24] through the inelastic light scattering and the photoluminescence of the surrounding 2DEG. In the recombination process following the optical pumping, a stable population of skyrmions is maintained in the 2DEG, which affects the nuclear polarization profile [96] and raises another computational difficulty.

In this work we report on detailed numerical studies of the coupling between the incompressible $\nu = 1$ and $\frac{1}{3}$ quantum Hall states and the localized nuclear spins. Following earlier discussion [74], we assume that the nuclear relaxation time is governed only by the hyperfine interaction with the electron spins. We find that the perturbation of the $\nu = 1$ or $\frac{1}{3}$ state by the hyperfine interaction with a localized spin results in the creation of a spin wave (SW) with a finite wave vector k and an energy $E(k)$ that is larger than the electronic Zeeman gap, $E(k) \geq E(0) = E_Z$. A spectral function for this process is calculated and shown to vanish at both $k = 0$ and $k \to \infty$. The maximum of the spectral function is at $k \sim 1/\lambda$, i.e. at the energy larger than $E(0) = E_Z$ by a term of the order of $E_C = e^2/\lambda$, and the nuclear Zeeman energy is much smaller than both E_C and E_Z. Therefore the energy conservation law prevents flipping nuclear spins at (locally) $\nu = 1$ or $\frac{1}{3}$, even if E_Z was made arbitrarily small. This explains long relaxation times observed in experiments.

At ν slightly different from 1 or $\frac{1}{3}$, the spin excitations coupled to a localized spin are the "internal excitations" of skyrmions in which their number of reversed spins K and angular momentum of a skyrmion change by one [33, 69, 125]. Remarkably, we find that the oscillator strength for this process increases with the skyrmion size K. Since the energy of the $K \to K + 1$ excitation is much smaller than E_Z (and, in particular, it can be made equal to the nuclear Zeeman gap at the appropriate value of E_Z), it means that the skyrmion-nucleus spin-flip processes will be allowed by the energy conservation law. This explains the shortened relaxation times of nuclear spin states at ν slightly different from 1 or $\frac{1}{3}$.

The dissertation is organized as follows. In Chap. 2 we discuss the details of the

theories of IQH and FQH effects, as well as the relation between the form of the Coulomb pseudopotential and the occurrence of the incompressible GS's in the lowest LL of an interacting 2DEG. In Chap. 3 we give an overview of the methods used in our calculations, that is the exact numerical diagonalization in Haldane's [36] spherical geometry based on a modified Lanczos [58] algorithm [44]. In Chap. 4 we report on our studies of the energy, interaction and photoluminescence of spin-reversed quasielectrons. A review of work done on spin excitations (spin waves and skyrmions) of a 2DEG in high magnetic fields can be found in Chap. 5. Finally, in Chap. 6 the reader will find the analysis of the hyperfine coupling of the localized nuclear spins to a 2DEG at $\nu = 1$ and $1/3$ and its effect on the nuclear spin relaxation processes.

Chapter 2

Quantum Hall Systems

2.1 Integral and Fractional Quantum Hall Effect

When a current I is passed in the x direction of a conductive sample in the presence of a magnetic field B along the z axis, there will be a Hall voltage $V_{\mathrm{H}} = \frac{BI}{ne}$ induced in the y direction (n is the number of moving carriers per unit area with charge $-e$). The Hall resistance, defined as $R_{\mathrm{H}} = V_{\mathrm{H}}/I$, is therefore expected to be linearly dependent on B. However, it was observed by von Klitzing *et al.* [55] that in high magnetic fields and low temperatures the function $R_{\mathrm{H}}(B)$ will have a number of plateaus, which could not be understood by means of classical theory.

In order to explain the quantized Hall plateaus let us first consider a two-dimensional gas of spinless electrons in a perpendicular magnetic field, which problem was initially solved by Landau [59]. In the Landau gauge, where the components of the vector potential are $A_x = -yB$ and $A_y = A_z = 0$, the Schrödinger equation for the wave function ψ and energy E reads

$$\frac{\hbar^2}{2m}\left\{\left[\frac{1}{i}\frac{\partial}{\partial x} - \frac{eB}{\hbar c}y\right]^2 - \frac{\partial^2}{\partial y^2}\right\}\psi = E\psi, \tag{2.1}$$

where m is the electron mass. The Hamiltonian does not depend explicitly on x and therefore the wave function can be written as $\psi = e^{ikx}\phi(y)$. Introducing the *magnetic*

length, $\lambda = (\hbar c/eB)^{\frac{1}{2}}$, we get

$$\frac{\hbar\omega_c}{2}\left\{-\lambda^2\frac{\partial^2}{\partial y^2}+\left[\frac{y}{\lambda}-\lambda k\right]^2\right\}\phi = E\phi. \tag{2.2}$$

This equation describes a shifted harmonic oscillator of the frequency ω_c. Its solution is therefore given by

$$\phi_{nk}(y) \propto H_n\left(\frac{y}{\lambda}-\lambda k\right)\exp\left[-\frac{(y-\lambda^2 k)^2}{2\lambda^2}\right], \tag{2.3}$$

where H_n is a Hermite polynomial of order n. The electronic energies fall into equally spaced and highly degenerate Landau levels (LL) numerated by $n = 0, 1, 2\ldots$ [60]

$$E_{nk} = \hbar\omega_c\left(n+\frac{1}{2}\right). \tag{2.4}$$

The degeneracy of LL is equal the number of flux quanta N_ϕ going through the allowed area C

$$N_\phi = \frac{BC}{\phi_0}, \tag{2.5}$$

where $\phi_0 = \frac{2\pi\hbar c}{|e|} = 4.135\times10^{-7}\text{Gauss}\cdot\text{cm}^2$ is a fundamental unit of magnetic flux (flux quantum).

The states ψ are extended in the x direction and confined in the y direction, however it is possible to find their linear combinations that are localized. Breaking the translational symmetry of the system lifts the LL degeneracy, which is essential for the occurrence of quantum Hall effect (QHE) [86]. Practically, this breakdown of symmetry is realized by introducing impurities or other imperfections. In such systems, the extended states lie very close to the unperturbed LL ($n\hbar\omega_c$) forming a conducting "core". The localized states, which cannot carry any current at zero temperature, lie in the energy gap between conducting cores. These levels are schematically presented in Fig. 2.1. When the Fermi energy is in the gap between the conducting cores, increasing the magnetic field (or the density of carriers) results in filling up the localized states without any change in the occupation of the extended ones, and hence without any effect on the Hall conductivity. This corresponds to the occurrence of plateaus in the Hall resistance and

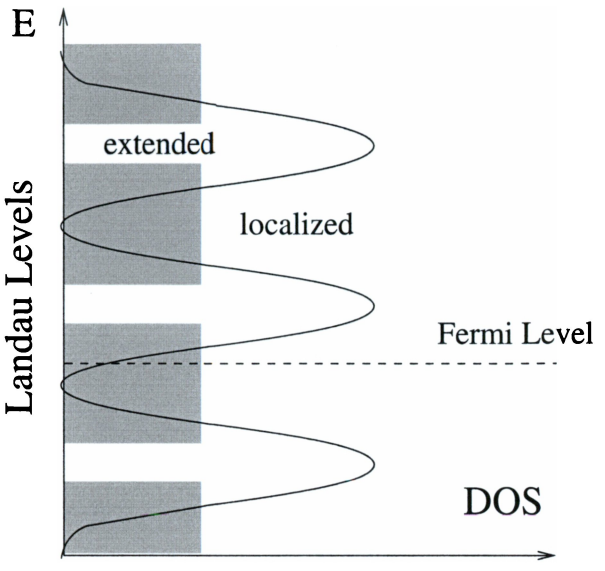


Figure 2.1: Density of states vs. energy E.

to the vanishing of the magneto-resistance (resistance in the x direction). Only when the Fermi level passes the core of extended states, the magneto-resistance becomes finite and the Hall resistance undergoes a transition from one plateau to another.

The observed plateaus occur at integral values of a *filling factor* defined as the total number of electrons N divided by LL degeneracy

$$\nu = \frac{N}{N_\phi} = \frac{nC}{BC/\phi_0} = \frac{nhc}{eB}, \tag{2.6}$$

where n is the number of electrons per unit area. This phenomenon is called the integral quantum Hall effect (IQHE).

The fractional quantum Hall effect (FQHE) has been discovered by Tsui *et al.* [108] in a high quality GaAs-$Al_xGa_{1-x}As$ heterostructures. It was found that in high magnetic fields and low temperatures there are plateaus in the Hall resistance and deep minima in the longitudinal resistance corresponding to a fractional filling of the lowest LL (here at $\nu = \frac{1}{3}$). The original results [108] showing the dependence of the Hall (ρ_{xy}) and longitudinal (ρ_{xx}) resistivities as functions of B and ν are presented in Fig. 2.2. These

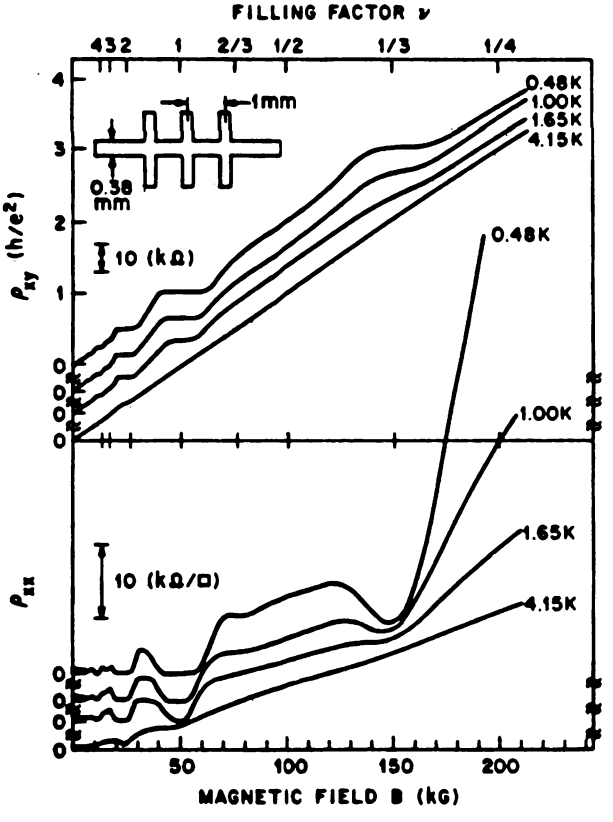


Figure 2.2: FQHE in the lowest LL at $\nu = \frac{1}{3}$ [108]. ρ_{xy} and ρ_{xx} are the Hall and longitudinal resistivities.

effects could not be explained by the IQHE theory, which suggested the existence of fractionally charged excitations.

Both IQHE and FQHE are a manifestation of the occurrence of non-degenerate incompressible ground states in the 2DEG at certain LL fillings, however the origins of the energy gaps responsible for these effects are not the same. In IQHE systems this is the single-particle cyclotron gap, whereas the gap responsible for FQHE is due to the repulsive interaction between particles, which leads to the formation of a new many-body ground state [62].

The original discovery by Tsui *et al.* [108] was followed by a number of experiments [18, 21, 28, 76, 77, 103], where the FQHE was observed for multiple series of filling factors $\nu \approx p/q$ (q is an odd number).

2.2 Laughlin Wave Function

In order to illustrate Laughlin's contribution to the theory of FQHE, let us consider a 2DEG in a perpendicular magnetic field in the rotationally invariant symmetric gauge ($\mathbf{A} = \frac{1}{2}[x\hat{y} - y\hat{x}]$) [60]. The solutions of the eigenvalue problem

$$\hat{H}\,|m,n\rangle = \hbar\omega_c \left(n + \frac{1}{2}\right) |m,n\rangle \tag{2.7}$$

can be written as

$$|m,n\rangle = \frac{1}{(2^{m+n+1}\pi m!n!)^{\frac{1}{2}}} e^{(1/4)(x^2+y^2)} \left[\frac{\partial}{\partial x} - i\frac{\partial}{\partial y}\right]^m \left[\frac{\partial}{\partial x} + i\frac{\partial}{\partial y}\right]^n e^{-(1/2)(x^2+y^2)}. \tag{2.8}$$

In the lowest LL

$$|m\rangle \equiv |m,0\rangle = \frac{1}{(2^{m+1}\pi m!)^{\frac{1}{2}}} z^m e^{-(1/4)|z|^2}, \tag{2.9}$$

where $z = x + iy$, and $|m\rangle$ is an angular momentum eigenstate corresponding to the eigenvalue m. A many-body Hamiltonian reads

$$\hat{H} = \sum_j \left\{ \left| \frac{\hbar}{i}\nabla_j - \frac{e}{c}\mathbf{A}_j \right|^2 + V(z_j) \right\} + \sum_{j>k} \frac{e^2}{|z_j - z_k|}, \tag{2.10}$$

where indices j and k go over N particles and V is the potential of the uniform background. Due to the quantization of the angular momentum, the average distance between electrons in FQHE takes on discrete values. Namely,

$$\left\langle m \left| r^2 \right| m \right\rangle = 2(m+1) \tag{2.11}$$

$$\left\langle m \left| \frac{1}{r} \right| m \right\rangle = \frac{(2m)!}{2^{2m+1}(m!)^2}\sqrt{2\pi} \to \frac{1}{\sqrt{2m}}. \tag{2.12}$$

Because the Coulomb interaction is small compared to the cyclotron energy, the many-body wave function can be approximated by a linear combination of antisymmetrized products of single-particle electron wave functions in the lowest LL. For two particles, the only wave functions which satisfy this condition and simultaneously describe the orbital motion with the relative angular momentum m (relative to the center of mass) are of the form

$$\psi = (z_1 - z_2)^m (z_1 + z_2)^n \exp\left[-\frac{1}{4}\left(|z_1|^2 + |z_2|^2\right)\right]. \tag{2.13}$$

Generalizing to the case of N particles

$$\psi(z_1, \ldots, z_n) = \text{const} \cdot \begin{vmatrix} 1 & z_1 & z_1^2 & \ldots & z_1^{N-1} \\ \ldots & & \ldots & \ldots & \ldots \\ 1 & z_N & z_N^2 & \ldots & z_N^{N-1} \end{vmatrix} \exp\left(-\sum_l^N \frac{|z_l|^2}{4}\right). \tag{2.14}$$

Laughlin's approximation [61, 62, 63] to the $\nu = \frac{1}{2p+1}$ state was the sequence of variational functions of the form of 2.14, in which the van der Monde determinant $\prod_{j<k}^N (z_j - z_k)$ was replaced by Jastrow factor $\prod_{j<k} (z_j - z_k)^m$ $(m = 2p+1)$ [62]:

$$|m\rangle = \psi_m(z_1, \ldots, z_N) = \prod_{j<k}^N (z_j - z_k)^m \exp\left(-\frac{1}{4}\sum_l^N |z_l|^2\right). \tag{2.15}$$

It can be shown [86] that for high electron densities the most stable has the wave function of a completely filled LL ($m = 1$), and with a decreasing density the states with $m = 3$, $m = 5$, etc. become stable. FQHE at $\nu = \frac{1}{3}$ corresponds to the first nontrivial state in this series ($m = 3$).

These incompressible ground state functions describe so-called *Laughlin correlations*, which refers to the tendency to avoid pair eigenstates with the largest repulsion in the low-energy many-body states. The elementary excitations of Laughlin states [62, 86, 108] can be understood in terms of quasiparticles (QP's) moving in the underlying incompressible state ("vacuum" or "reference" state). QP's have such single-particle properties as energy, LL degeneracy and (fractional) electric charge of $\pm(2p+1)^{-1}e$. There are two types of Laughlin QP's, corresponding to an excessive (quasihole QH) or missing (quasielectron QE) single-particle state compared to an exact $\nu = \frac{1}{(2p+1)}$ filling. Their functions can be obtained by multiplying Eq. 2.15 by $\prod_k \partial/\partial z_k$ and $\prod_k z_k$ for QE's and QH's, respectively.

More generally, Laughlin correlations occur when the Hilbert space is degenerate and the two-body repulsive interaction has short range [119]. These correlations were shown to exist in a number of different systems [117, 118], in particular in a system of Laughlin QP's [64], which gave rise to the hierarchy theory [132]. In this model, a sequence of successive incompressible *daughter* states is derived from a *parent* state of filling $\nu = \frac{1}{2p+1}$ [36, 41, 64]. The filling factors of the daughter states are given by the formula

$$f = \left(m + \frac{\alpha_1}{p_1 + \frac{\alpha_2}{p_2 + \ldots \frac{\alpha_n}{p_n}}} \right), \tag{2.16}$$

where $\alpha_i = \pm 1$, and p_i is even.

2.3 Composite Fermion Picture

The fractional statistics of QP's can be interpreted by means of the Chern-Simons (CS) transformation, which was introduced to the analysis of FQHE by Lopez *et al.* [67] and Halperin *et al.* [42] and to the theory of even-denominator filling factors by Kalmeyer *et al.* [50]. In CS transformation a fictitious magnetic flux tube oriented opposite to the original magnetic field B is attached to each electron. The composite particles obtained in this way carry electric charge and magnetic flux. The CS transformation is

a gauge transformation and therefore the energy spectrum remains unchanged. The classical equation of motion is also unchanged because the fluxes do not penetrate the occupied area. However, there is an additional term in the quantum Hamiltonian describing the charge–flux interaction resulting in a Aharonov-Bohm phase [1], acquired when an electron encircles a magnetic flux. Therefore the number of flux quanta attached to electrons determines the statistics of the composite particles. If the number of flux quanta is even ($2p$), the CS transformation describes the formation of composite fermions (CF's).

The CS interaction Hamiltonian contains two- and three-body terms and in this model there is no small parameter that would allow to treat this problem perturbatively. The solution proposed by Jain [46] is based on the mean-field approximation in which the magnetic field due to attached flux tubes is spread evenly over the occupied area C. The effective magnetic field B^* seen by the mean-field CF's is lower than the original field B seen by electrons by a term $2p\phi_0 N/C = B - B^*$. An effective CF filling factor ν^* is defined as

$$(\nu^*)^{-1} = \nu^{-1} - 2p, \tag{2.17}$$

so that

$$B^*\nu* = B\nu = \frac{N}{C}\phi_0. \tag{2.18}$$

The mean-field Hamiltonian of non-interacting CF's gives a good qualitative description of the low-lying states of strongly interacting electrons in their lowest LL. In this mapping the $\nu^* = n$ state (where n is an integer) corresponds to the series of FQHE states at $\nu = \frac{n}{1+2pn}$ [47]. If ν^* is not an integer, the low-lying states contain a number of QP's moving in the incompressible state with integer ν^*.

2.4 Coulomb Pseudopotential and Composite Fermion Picture

Despite of the success of the mean-field CF approach in describing the low-energy spectrum of finite systems and in predicting filling factors at which the FQHE has been experimentally observed, the question why this model works is not trivial at all. The original conjecture of Jain [47] that a system of strongly interacting electrons can be mapped onto a weakly interacting system of CF's is based on the assumption that the Coulomb interactions and CS fluctuations beyond the mean-field tend to cancel each other leaving a small residual interaction between CF's. This reasoning cannot be correct because the CS interactions between fluctuations are measured on an energy scale proportional to $\hbar\omega_c \propto B$, which can be much larger than the energy scale of the Coulomb interactions, proportional to $e^2/\lambda \propto B^{1/2}$ [117, 119].

The CF picture fails when applied to a number of cases in which identical charged fermions interact through a Coulomb-like potential. Only some of the filling factors predicted by this theory describe incompressible states for such systems as Laughlin QP's in the FQH hierarchy [36, 41, 64], for the CF's themselves in the CF hierarchy [97], and for electrons in the lowest LL, when the layer thickness exceeds certain critical value [94]. The CF picture can be used to make certain predictions in the systems known to be incompressible and to have Laughlin-like correlations, however it cannot predict its own validity for such a system [119]. It has been shown [120, 122] that it is the knowledge of the Coulomb pseudopotential that is necessary to predict the type of correlations (and possible incompressibility) in a given many-body system.

The two-body interaction Hamiltonian in the many-body system can be written as

$$\hat{H} = \sum_{i<j} \sum_{L} V(L) \hat{\mathcal{P}}_{ij}(L). \tag{2.19}$$

Here, $V(L)$ is the two-particle interaction pseudopotential [38, 39, 86] defined as the interaction energy of a pair in an isolated LL labeled by the pair angular momentum L,

$$\hat{H} \left| L \right\rangle = V(L) \left| L \right\rangle \tag{2.20}$$

and $\hat{\mathcal{P}}_{ij}(L)$ is the projection operator onto the subspace with the pair ij in the state $|L\rangle$. Because the number of single-particle states in the lowest LL is limited, the number of pair states is also limited and the electron-electron interaction potential enters the Hamiltonian 2.19 only through a small set of pseudopotential parameters $V(\mathcal{R})$. $\mathcal{R}$ is the relative angular momentum

$$\mathcal{R} = |L - L_{\mathrm{cd}}|\,, \tag{2.21}$$

where L_{cd} is the angular momentum of a *compact droplet*, that is a configuration of particles occupying the most inner orbitals (here $L_{\mathrm{cd}} = 1$). Using the relative angular momentum $\mathcal{R}$ instead of the eigenvalue L of total angular momentum to label pair states and pseudopotential coefficients will allow a comparison of the pseudopotentials in a planar system and in a spherical system exploited by us in numerical experiments (see Sec. 3.3). Each pair state corresponds to a certain average electron separation d, and $\mathcal{R} \propto d$. A large slope $\mathrm{d}V/\mathrm{d}\mathcal{R}$ means a large energy gradient, that is a large effective force between two point charges at a distance d.

Let us define a model *hard core* pseudopotential V_{HC} [115]

$$\begin{aligned} V_{\mathrm{HC}}(\mathcal{R}) &\gg V_{\mathrm{HC}}(\mathcal{R}+2) \\ V_{\mathrm{HC}}(\mathcal{R}-2) - V_{\mathrm{HC}}(\mathcal{R}) &\gg V_{\mathrm{HC}}(\mathcal{R}) - V_{\mathrm{HC}}(\mathcal{R}+2) \end{aligned} \tag{2.22}$$

for all values of $\mathcal{R}$. The lowest-energy many-body states are realized by a configuration of particles at maximum possible separation (minimum repulsive potential), which in the language of the discussed formalism means avoiding pair states with lowest $\mathcal{R}$. The V_{HC} is an ideal short-range pseudopotential which yields Laughlin correlations and incompressibility of a given many-body system [115]. The important question is whether the states corresponding to vanishing of pseudopotential coefficients with the lowest values of $\mathcal{R}$ are the eigenstates of the actual (not strictly hard-core) interaction pseudopotential (e.g. Coulomb interaction in a given LL) and whether they have low energy. In other words, what is the condition for $V(\mathcal{R})$ to act like hard-core repulsion and to have the energy spectrum characteristic of the FQH effect.

It has been shown [115] that the condition for the occurrence of the Laughlin correlations and thus incompressible states is that the pseudopotential $V(\mathcal{R})$ decreases more quickly than the harmonic pseudopotential $V_{\rm H}$, which on a plane is a linear function of $\mathcal{R}$. For example, the Coulomb pseudopotential for the lowest LL was shown to have this property in the entire range of $\mathcal{R}$. As a result, the low-energy states are those with vanishing pseudopotential coefficients for a certain number of lowest values of $\mathcal{R}$ and these states are the incompressible $\nu = (2p+1)^{-1}$ states. This explains the success of Jain's CF picture when applied to these systems. The pseudopotential formalism gives a clear criterion for incompressibility of spin polarized states and clarifies why in some cases the mean-field CF picture fails, which is discussed in detail in Ref. [119]. For instance, the CF hierarchy uses the mean-field approach for the QP's and therefore should fail unless the QP pseudopotential has a short-range nature, as defined in this section. It was found that QP's have Laughlin correlations at some of the Laughlin filling factors but not at others, which for example explains incompressibility of hierarchy ground states at $\nu = \frac{2}{7}$ and compressibility at such hierarchy fractions as $\nu = \frac{4}{7}$ or $\nu = \frac{4}{13}$.

2.5 Composite Fermions with a Spin Freedom

It has been shown by Yoshioka [133] that the CF transformation can be applied also to systems in which the electrons are partially spin-polarized. A set of rules for such transformation was derived for a various series of filling factors assuming that the magnetic field B is large so that only the lowest LL for each polarization need be considered. Due to the electron-hole symmetry, the states $\nu' = 2 - \nu$ and ν are equivalent. It was shown that the electronic $\nu = \frac{p}{mp+1}$ filling factors (p is an integer and m is an even integer) can be mapped into a CF system at $\nu^* = p$ by attaching m number of fluxes to each electron. The effective field of CF equals $B^* = \frac{B}{mp+1}$ and the lowest LL of each spin is split into $mp+1$ CF LL. On the other hand, the filling factors of the form $\nu = 1 + \frac{p}{mp+1}$ (or equivalently $\nu' = 1 - \frac{p}{mp+1}$) correspond to a CF filling factor $\nu^* = |mp+1| + |p|$,

which results from the application of the following rules: (i) CF are formed by attaching m flux quanta to each electron. (ii) Each electron in the lower energy spin-$\downarrow$ LL gives $|m|$ flux quanta with opposite signs. (iii) The maximum allowed CF filling factor for each spin state is $|mp+1|$. (iv) The effective magnetic field seen by CF's is $B^* = \frac{B}{mp+1}$.

These rules give the foundation for the experimental determination of the mass and g-factor of CF's [130].

Chapter 3

Numerical Studies

3.1 Haldane Sphere

As discussed in Sec. 2.1, the measure of density of 2DEG in a magnetic field is given by the filling factor ν defined by Eq. 2.6. In the absence of electron-electron interactions, the N_ϕ single-particle states are degenerate (see Eq. 2.5). Because these interactions entirely dominate the low-energy spectrum at $\nu < 1$, they cannot be treated perturbatively. Since the Hamiltonian including the interaction term is not analytically soluble, a number of numerical diagonalization techniques have been commonly employed, which however limit the system to a finite (small) number of electrons. To model an infinite 2DEG at a finite density, such approaches have been used as imposing a lateral (parabolic, hard wall, etc.) confinement [62], periodic boundary conditions [38], or confining electrons on a closed surface [36]. The main advantages of the last approach are that it naturally avoids edge effects and that the translational symmetry of a (planar) 2DEG is preserved in the form of the rotational symmetry on a sphere. In particular, the pair of good quantum numbers on a plane, the center of mass and relative momenta, correspond to the pair of good quantum numbers on the sphere–the projection L_z and the total L angular momenta [4, 116]. Consequently, the degeneracies associated with the center-of-mass excitations on a plane correspond to those associated with differ-

ent values of L_z on a sphere, and the non-degenerate incompressible states in a planar system have their counterparts in non-degenerate ($L = 0$) states on a sphere [119].

Let us consider N non-interacting electrons on the Haldane sphere of radius R. The magnetic field B normal to the surface is due to a Dirac monopole [25]. The monopole strength $2Q$ is defined in the units of flux quantum ϕ_0 (Eq. 2.5), so that the total flux through the sphere is $4\pi BR^2 = 2Q\phi_0$ ($2Q$ is an integer). The Hamiltonian of an electron with an effective mass μ moving on the surface of Haldane sphere reads

$$H = \frac{1}{2\mu}\left(\mathbf{p} + \frac{e}{c}\mathbf{A}\right)^2 = \frac{\mathbf{\Lambda}^2}{2\mu R^2}, \tag{3.1}$$

where $\mathbf{p} = -i\hbar\nabla$, and $\mathbf{\Lambda}$ is the dynamical angular momentum

$$\mathbf{\Lambda} = \mathbf{r} \times \left(-i\hbar\nabla + \frac{e}{c}\mathbf{A}\right) \tag{3.2}$$

with $\mathbf{A}$ being a vector potential. In the presence of a magnetic field $B = \frac{c\hbar Q}{eR^2}$ the operator $\mathbf{\Lambda^2}$ is not a rotation generator, which can be seen by evaluating the commutation relations:

$$\begin{aligned}
[\Lambda_\alpha, \Lambda_\beta] &= \left[M_\alpha + \varepsilon_{\alpha\mu\nu} r_\mu \frac{e}{c} A_\nu, M_\beta + \varepsilon_{\beta tu} r_t \frac{e}{c} A_u\right] \\
&= i\hbar\varepsilon_{\alpha\beta\gamma} M_\gamma - i\hbar\frac{e}{c}\varepsilon_{\alpha\mu\nu}\varepsilon_{\beta tu}\left\{[r_\mu A_\nu, r_t\partial_u] + [r_\mu\partial_\nu, r_t A_u]\right\} \\
&= i\hbar\varepsilon_{\alpha\beta\gamma} M_\gamma - i\hbar\frac{e}{c}\left\{\left(\delta_{\alpha\beta}\delta_{\mu\nu} - \delta_{\alpha u}\delta_{\mu\beta}\right)\left(r_u A_\mu - r_\mu A_u\right) + \varepsilon_{\alpha\mu\nu}\varepsilon_{u\eta\nu}\varepsilon_{\beta tu} r_t r_\mu B_\eta\right\} \\
&= i\hbar\varepsilon_{\alpha\beta\gamma} M_\gamma + i\hbar\frac{e}{c}\varepsilon_{\alpha\beta\gamma}\left(\mathbf{r}\times\mathbf{A}\right)_\gamma - i\hbar\frac{e}{c}\left(\delta_{\alpha u}\delta_{\mu\eta} - \delta_{\alpha\eta}\delta_{\mu u}\right)\varepsilon_{\beta tu} r_t r_\mu B_\eta \\
&= i\hbar\varepsilon_{\alpha\beta\gamma}\left(\Lambda_\gamma - \hbar Q\Omega_\gamma\right).
\end{aligned} \tag{3.3}$$

Here, $M_\alpha = -i\hbar\varepsilon_{\alpha\beta\gamma} r_\beta\partial_\gamma$ ($|r| = R$) stands for the angular momentum in the absence of B and

$$\hat{\Omega}(\theta,\phi) = \hat{r} = \frac{\mathbf{r}}{R} \tag{3.4}$$

is the unit vector in spherical coordinates (r, θ, ϕ).

Noticing that

$$[\Lambda_\alpha, \Omega_\beta] = -i\frac{\hbar}{R}\varepsilon_{\alpha\mu\nu}\left[r_\mu\partial_\nu, r_\beta\right] = i\hbar\varepsilon_{\alpha\beta\mu}\Omega_\mu, \tag{3.5}$$

one can construct the operator $\mathbf{l}$

$$\mathbf{l} = \mathbf{\Lambda} + \hbar Q \hat{\Omega}, \tag{3.6}$$

and show that its components satisfy the proper commutation relations

$$[l_\alpha, l_\beta] = i\hbar\varepsilon_{\alpha\beta\gamma}\left(\Lambda_\gamma - \hbar Q\Omega_\gamma\right) + 2i\hbar^2 Q\varepsilon_{\alpha\beta\gamma}\Omega_\gamma = i\hbar\varepsilon_{\alpha\beta\gamma}l_\gamma. \tag{3.7}$$

Therefore the operators $\mathbf{l}$ is the *generator of infinitesimal rotations* and the eigenvalues of $\mathbf{l}^2$ are of the form $\hbar^2 l(l+1)$. The relation $\mathbf{\Lambda}\cdot\mathbf{\Omega} = \mathbf{\Omega}\cdot\mathbf{\Lambda}$ =0 gives $\mathbf{l}\cdot\hat{\Omega} = \hat{\Omega}\cdot\mathbf{l} = \hbar S$ and thus the Hamiltonian 3.1 can be rewritten as

$$H = \frac{1}{2\mu R^2}\left(\mathbf{l}^2 - \hbar^2 Q^2\right), \tag{3.8}$$

with corresponding eigenenergies

$$\varepsilon_l = \frac{\hbar^2}{2\mu R^2}\left[l(l+1) - Q^2\right]. \tag{3.9}$$

The eigenvalues Λ^2 are positive, hence $l \geq Q$.

The common eigenfunctions of the single-particle Hamiltonian, the angular momentum $\mathbf{l}$ and its projection l_z are called *monopole harmonics* [37, 126] and are denoted here as $|Q,l,m\rangle$ (or in the simplified form $|m\rangle$):

$$\begin{aligned}
\mathbf{l}^2\,|Q,l,m\rangle &= \hbar^2 l(l+1)\,|Q,l,m\rangle\,, \\
l_z\,|Q,l,m\rangle &= \hbar m\,|Q,l,m\rangle\,, \\
H\,|Q,l,m\rangle &= \frac{\hbar\omega_c}{2Q}\left[l(l+1) - Q^2\right]|Q,l,m\rangle\,.
\end{aligned} \tag{3.10}$$

The degenerate angular momentum shells are equivalent to the LL's of the planar geometry and are enumerated by $n = l - Q$ ($n = 0, 1, \ldots$). Therefore the eigenenergies 3.9 can be written in the form

$$\varepsilon_n = \hbar\omega_c\left(n + \frac{1}{2} + \frac{n(n+1)}{2Q}\right) = E_0\left[2Q\left(n + \frac{1}{2}\right) + n(n+1)\right], \tag{3.11}$$

where the cyclotron frequency equals $\omega_c = \frac{eB}{\mu c} = \frac{Q\hbar}{\mu R^2}$ and $E_0 = \frac{\hbar\omega_c}{2Q} = \frac{\hbar^2}{2\mu R^2}$ is a B-independent energy scale. The lowest LL on a sphere corresponds to $l = Q$ ($n = 0$)

and its degeneracy equals $N_\phi = 2l+1$. When all single-particle states are occupied, the electron density

$$\frac{2Q+1}{4\pi R^2} \sim \frac{Q}{2\pi R^2} = \frac{1}{2\pi\lambda^2}, \tag{3.12}$$

where $\lambda = \frac{R}{\sqrt{Q}}$ is the magnetic length (see Sec. 2.1). A comparison with Eq. 2.6 shows that for large Q (large R) the densities of the lowest LL on a plane and on a sphere are equal.

In spherical coordinates the components of $\mathbf{l}$ ($\mathbf{l}^2 = l_z^2 + \frac{1}{2}(l^+l^- + l^-l^+)$) read

$$\begin{aligned} l^\pm = l_x \pm i l_y &= \hbar e^{\pm i\phi}\left(\pm\partial_\theta + \frac{\cos\theta}{\sin\theta} i\partial_\phi + Q\frac{1-\cos\theta}{\sin\theta}\right), \\ &= \hbar e^{\pm i\phi}\left(\mp 2\sqrt{\oplus\ominus}\partial_x + \frac{1}{2}\left(\sqrt{\oplus/\ominus} - \sqrt{\ominus/\oplus}\right) i\partial_\phi + Q\sqrt{\ominus/\oplus}\right), \\ l_z &= \hbar(-i\partial_\phi + Q), \end{aligned} \tag{3.13}$$

where

$$x = \cos\theta, \quad \oplus = \frac{1+x}{2} = \cos^2\frac{\theta}{2}, \quad \ominus = \frac{1-x}{2} = \sin^2\frac{\theta}{2}. \tag{3.14}$$

The monopole harmonics can be thus written explicitly

$$Y_{Q,n,m}(\hat{\Omega}) \equiv \left\langle \hat{\Omega} | Q, n, m \right\rangle = N_{Q,n,m} \sqrt{\ominus}^{Q-m} \sqrt{\oplus}^{Q+m} P_n^{Q-m,Q+m}(x) e^{i(m-Q)\phi}, \tag{3.15}$$

where

$$N_{Q,n,m}^2 = \frac{2l+1}{4\pi} \cdot \frac{\begin{pmatrix} 2l \\ l+m \end{pmatrix}}{\begin{pmatrix} 2l \\ l+Q \end{pmatrix}} \tag{3.16}$$

is a normalization constant, and $P_n^{\alpha,\beta}$ is the Jacobi polynomial of the nth order:

$$P_n^{\alpha,\beta}(x) = \sum_{q=0}^{n} (-1)^q \begin{pmatrix} n+\alpha \\ n-q \end{pmatrix} \begin{pmatrix} n+\beta \\ q \end{pmatrix} \oplus^{n-q} \ominus^q \equiv \sum_q c_{n,q}^{\alpha,\beta} \oplus^{n-q} \ominus^q. \tag{3.17}$$

Jacobi polynomials are generalized Legendre functions which can be obtained from Eq. 3.17 by setting $q = 0$ and $\alpha = \beta$, which in turn corresponds to $Q = 0$. The relation

between the spherical harmonics $Y_{n,m}$ and monopole harmonics (generalized spherical harmonics) is therefore $Y_{n,m} = Y_{0,n,m}$.

Rotation of a monopole harmonic differs from that of a usual spherical harmonic by a phase factor α dependent only on the rotation and Q, and independent of l, m or μ [31]:

$$\begin{aligned} \hat{\mathcal{D}}\, Y_{S,n,m}(\hat{\Omega}) &= Y_{S,n,m}(\hat{\mathcal{D}}^{-1}\hat{\Omega}) = e^{i\alpha} \sum_{\mu} \mathcal{D}^{l}_{\mu,m}\, Y_{S,n,\mu}(\hat{\Omega}), \\ \hat{\mathcal{D}}\, Y^{*}_{S,n',m'}(\hat{\Omega})\, Y_{S,n,m}(\hat{\Omega}) &= \sum_{\mu',\mu} \mathcal{D}^{l'*}_{\mu',m'} \mathcal{D}^{l}_{\mu,m}\, Y^{*}_{S,n',\mu'}(\hat{\Omega})\, Y_{S,n,\mu}(\hat{\Omega}). \end{aligned} \tag{3.18}$$

$\hat{\mathcal{D}}$ is the rotation operator and its matrix elements are the Wigner functions [93]

$$\hat{\mathcal{D}}^{l}_{\mu,m}(\mathbf{r}) = \left\langle l,\mu \left| \exp\left(\frac{-i\mathbf{l}}{\hbar}\right) \right| l,m \right\rangle. \tag{3.19}$$

The operator $\hat{\mathcal{D}}$ has a particularly useful form for the rotation of $\hat{\Omega}_1 = \hat{\Omega}(\theta,\phi)$ to $\hat{N} = \hat{\Omega}(0,0)$, because then it becomes a special case of the Euler rotation operator $\hat{\mathcal{D}}(\gamma,-\theta,-\phi)$ (γ, θ, ϕ are Euler angles [93]). Choosing $\gamma = 0$, we have

$$\begin{aligned} \mathcal{D}^{l}_{\mu,m} &\equiv \mathcal{D}^{l}_{\mu,m}(0,-\theta,-\phi) = e^{im\phi} d^{l}_{\mu,m}(-\theta), \\ d^{l}_{\mu,m}(-\theta) &= \sum_{\substack{\alpha\geq 0 \\ \alpha\geq m-\mu}}^{\substack{\alpha\leq l+m \\ \alpha\leq l-\mu}} \xi^{l,\alpha}_{\mu,m} \cos^{2l-2\alpha-\mu+m}(-\theta/2) \sin^{2\alpha+\mu-m}(-\theta/2) \\ &= (-1)^{\mu-m} \sum_{\substack{\alpha\geq 0 \\ \alpha\geq m-\mu}}^{\substack{\alpha\leq l+m \\ \alpha\leq l-\mu}} \xi^{l,\alpha}_{\mu,m} \sqrt{\oplus}^{2l-2\alpha-\mu+m} \sqrt{\ominus}^{2\alpha+\mu-m}; \\ \xi^{l,\alpha}_{\mu,m} &= (-1)^{\alpha+\mu-m} \sqrt{\binom{l+\mu}{\alpha+\mu-m}\binom{l-\mu}{\alpha}\binom{l+m}{\alpha}\binom{l-m}{\alpha+\mu-m}}. \end{aligned} \tag{3.20}$$

3.2 Many-Body States

For convenience, in our numerical calculations the many-body Hilbert space is spanned by single-particle configurations (Slater determinants) $|m_1, m_2, \ldots, m_N\rangle$, which are labeled by the projection of total angular momentum $M = m_1 + m_2 + \ldots + m_N$. These

are $N_{\rm MB} = N_\phi! \, [N!(N_\phi - N)!]^{-1}$-fold degenerate antisymmetric N electron states of a given (N_ϕ-fold degenerate) LL. Taking advantage of the Wigner-Eckart theorem, each (M) Hilbert subspace can be further block-diagonalized into (M, L) Hilbert subspaces corresponding to different values of the total angular momentum L. The Wigner-Eckart theorem applied here says that the matrix elements of the scalar interaction Hamiltonian between angular momentum eigenstates $|L, M, \alpha\rangle$ can be written as

$$\langle L', M', \alpha' \, | H | \, L, M, \alpha \rangle = \delta_{LL'} \delta_{MM'} V_{\alpha\alpha'}(L), \tag{3.21}$$

where

$$V_{\alpha\alpha'}(L) = \langle L, \alpha' \, | V | \, L, \alpha \rangle \, , \tag{3.22}$$

is the M-independent reduced matrix element and the index α distinguishes different states in the same (M, L) Hilbert space. The Coulomb matrix elements in the bases $|m_1, m_2, \ldots, m_N\rangle$ and $|L, M\rangle$ are related through the Clebsch-Gordan coefficients. V is the two-body Coulomb interaction and hence the object of our numerical studies is to diagonalize the electron-electron Hamiltonian

$$H = \sum_{m_1 m_2 m_3 m_4} c^\dagger_{m_1} c^\dagger_{m_2} c_{m_3} c_{m_4} \, \langle m_1, m_2 \, | V | \, m_3, m_4 \rangle \, . \tag{3.23}$$

The two-body Coulomb matrix elements which appear in this Hamiltonian have a particularly simple form in the lowest LL [31], but they can also be evaluated analytically for a general case of inter- or intra-LL scattering. Introducing the notation

$$\begin{aligned} I^{n_1,m_1}_{n_2,m_2}(k_1, k_2) &= \left\langle n_1, m_1 \left| \oplus^{k_1} \ominus^{k_2} \right| n_2, m_2 \right\rangle_x \\ &= 2\pi \int_{-1}^{+1} dx \, Y_{S,n_1,m_1}(x) \; \oplus^{k_1} \ominus^{k_2} \; Y_{S,n_2,m_2}(x) \end{aligned} \tag{3.24}$$

(where $k_1 = \alpha_2 + \alpha_3 + (\mu_2 - m_2 + \mu_3 - m_3)/2$, $k_2 = l_2 + l_2 - k_1$, and $\oplus$, $\ominus$, ξ and α are defined through Eqs. 3.14, 3.18–3.20), one can show that the Coulomb matrix elements equal:

$$\left\langle H^{(C)} \right\rangle = \frac{e^2}{R} \left\langle n_1, m_1; n_2, m_2 \left| |\hat{\Omega}_1 - \hat{\Omega}_2|^{-1} \right| n_3, m_3; n_4, m_4 \right\rangle =$$

Table 3.1: The dimension N_ϕ of the single particle Landau level, dimension $N_{\rm MB}$ of the total many body Hilbert space, dimension $N_{\rm MB}(0)$ of the largest (M) subspace, dimension $N_{\rm MB}^{\rm MAX}(M,L)$ of the largest (M,L) subspace and dimension $N_{\rm MB}(0,0)$ of the (M,L) subspace containing the Laughlin $L=0$ ground state, of $N=6$ to 11 electrons at the filling factor $\nu=\frac{1}{3}$ [119].

N	N_ϕ	$N_{\rm MB}$	$N_{\rm MB}(0)$	$N_{\rm MB}^{\rm MAX}(M,L)$	$N_{\rm MB}(0,0)$
6	16	8,008	338	24	6
7	19	50,388	1,656	86	10
8	22	319,770	8,512	352	31
9	25	2,042,975	45,207	1,533	84
10	28	13,123,110	246,448	7,069	319
11	31	84,672,315	1,371,535	33,787	1,160

$$= \frac{e^2}{R}\left\langle n_1,m_1\left|\left\langle n_2,m_2\left|\frac{1}{2(1-\cos(\theta_1-\theta_2))}\right|n_3,m_3\right\rangle\right|n_4,m_4\right\rangle = \quad (3.25)$$

$$= \frac{e^2}{R}\delta^{m_1+m_2}_{m_3+m_4}\sum_{\mu_2,\mu_3}\delta^{\mu_2}_{\mu_3}I^{n_2,\mu_2}_{n_3,\mu_3}(0,-1/2)\sum_{\alpha_2,\alpha_3}\xi^{l_2,\alpha_2}_{\mu_2,m_2}\xi^{l_3,\alpha_3}_{\mu_3,m_3}I^{n_1,m_1}_{n_4,m_4}(k_2,k_1).$$

We evaluate these matrix elements numerically.

A diagonalization of the Hamiltonian 3.23 gives the eigenenergies E as a function of the total angular momentum L. The numerical results for the lowest LL always show one or more L multiplets forming a low-energy sector. Typical dimensions of Hilbert subspaces are given in Ref. [119] and cited here in Table 3.1.

3.3 Mean-Field Composite Fermion Picture in Spherical Geometry

In the mean-field CF picture the vector potential due to the evenly spread electrons with attached flux tubes, produces and isotropic magnetic field (Sec. 2.3). It is identical to that of a magnetic monopole of strength $-2pN$ placed at the center of Haldane sphere. However, since an electron does not interact with its own flux, one has make a correction

so that the effective monopole strength is

$$2Q^* = 2Q - 2p(N-1), \tag{3.26}$$

where $l^* = |Q^*|$ plays the role of the angular momentum of the lowest CF shell [20].

The N-electron incompressible state at $2Q$ correspond to n lowest CF LL at $2Q^*$ completely filled by N CF's. The states at other values of $2Q$ are compressible and contain $N_{\rm QP}$ QP's in the neighboring incompressible state at $2Q_{\rm inc}$,

$$\begin{aligned} N_{\rm QP} &= n\left(|2Q^*_{\rm inc}| - |2Q^*|\right), \\ &= n\left(|2Q_{\rm inc} - 2p_{\rm inc}(N-1)| - |2Q - 2p(N-1)|\right), \end{aligned} \tag{3.27}$$

where $2p$ and $2p_{\rm inc}$ are the flux strengths applied in CS transformation to the states at $2Q$ and $2Q_{\rm inc}$, respectively. Since the numbers $2p$ and $2p_{\rm inc}$ do not have to be equal, alternative pictures of the $(N, 2Q)$ state, containing different QP's, can be obtained [131]. All values of $2Q$ that lead to the same value of $l^* = Q^*$ are equivalent and their low-energy spectrum contain the same L multiplets.

As discussed in Sec. 2.4, the condition for the occurrence of the Laughlin correlations and incompressible states is that the pseudopotential $V(\mathcal{R})$ decreases more quickly than the harmonic pseudopotential $V_{\rm H}$. On a sphere, the relative angular momentum equals (Eq. 2.21)

$$\mathcal{R} = 2l - L, \tag{3.28}$$

where $\mathbf{L} = \mathbf{l_1} + \mathbf{l_2}$ is the angular momentum of a pair of fermions at the averaged distance d. It can be also shown [119] that within the nth LL of the Haldane sphere

$$\frac{d^2}{R^2} = 2 + \frac{Q^2}{l(l+1)}\left(2 - \frac{L^2}{l(l+1)}\right), \tag{3.29}$$

and therefore, similarly as on a plane, larger $\mathcal{R}$ means larger separation d. In spherical geometry, for the harmonic repulsive interaction $V_{\rm H}$ within an isolated LL, the energy increases linearly with increasing $L(L+1)$. Hence one can introduce a model pseudopotential [115]

$$V_\beta(L) = [L(L+1)]^\beta, \tag{3.30}$$

where the exponent β is the relevant measure of the *short range* (hard-core) character of a pseudopotential V_β. The low-lying states of interacting many-body system at $\nu \approx (2p+1)^{-1}$ tend to have Laughlin correlations ($V(\mathcal{R}) \approx 0$ for $\mathcal{R} < 2p-1$), if the pseudopotential $V(\mathcal{R})$ decreases for all values of $\mathcal{R}$ and decreases more quickly than the harmonic pseudopotential $V_{\rm H}$ in the vicinity of $\mathcal{R} = 2p+1$ ($\beta > 1$ in Eq. 3.30) [119].

Chapter 4

Energy, Interaction and Photoluminescence of Spin-Reversed Quasielectrons

4.1 Introduction

It is quite remarkable that the most prominent FQH states, the Laughlin ground states [62] that occur at $\nu = (2p+1)^{-1}$ (p is an integer), are the only ones that are maximally spin-polarized solely due to the electron–electron exchange interaction. At other filling factors, the 2DEG is known [3, 14, 17, 40, 127, 128, 134] to be at least partially unpolarized unless the Zeeman energy E_Z is sufficiently large. Only partial polarization of the FQH states at the filling factors other than $\nu = (2p+1)^{-1}$ causes transitions [16] between incompressible and compressible or different incompressible phases as a function of E_Z, realized in tilted-field experiments [22, 29, 30, 112]. The finite excitation gap Δ of the Laughlin state results from the finite energies ε of its elementary charge excitations, Laughlin quasielectrons (QE's) and quasiholes (QH's), as well as from the lack of the particle–hole symmetry between them that causes a magneto-roton type of dispersion of the QE–QH interaction with a minimum at a finite wave vector k. Indeed, the cal-

culated [31, 37, 38, 64, 119] energy $\varepsilon_{\mathrm{QE}} + \varepsilon_{\mathrm{QH}}$ needed to create a spatially separated QE–QH pair necessary for electric current agreed reasonably well with the activation energy obtained from the temperature dependences of the FQHE at $\nu = (2p+1)^{-1}$.

Therefore, it was quite surprising when Rezayi [91] and Chakraborty *et al.* [15] discovered that another low-energy excitation of the Laughlin state exists, a spin-density wave, which becomes gapless at $E_{\mathrm{Z}} = 0$. It turns out that it is only due to a finite Zeeman energy that the spontaneous creation of spin waves, each consisting of a positively charged QH and a negatively charged reversed-spin quasielectron ($\mathrm{QE_R}$), does not destroy incompressibility of Laughlin states in the experimental 2DEG systems. Although the spin excitations of Laughlin states have been extensively studied in the context of the real-space spin patterns called skyrmions [66, 102] (see Chap. 5), our knowledge of their interaction with one another or with other excitations, or their optical properties is not yet complete (specially at fractional ν). In this chapter we address both of these issues. The results have been published in Ref. [105, 106].

First, we identify QE, QH, and $\mathrm{QE_R}$ as the three elementary quasiparticles (QP's) of a Laughlin state and determine their mutual interaction pseudopotentials $V(\mathcal{R})$ (Sec. 2.4). For example, the $\mathrm{QE_R}$–$\mathrm{QE_R}$ pseudopotential is found to be very different from the QE–QE pseudopotential at short range, which is the reason for incompressibility of a partially polarized $\nu = \frac{4}{11}$ state at low E_{Z} (in contrast to the compressible [120] fully polarized state at the same ν). A partially polarized $\nu = \frac{4}{11}$ state has been also recently proposed by Park and Jain [85] within a composite fermion model. However, their interpretation of the $\nu = \frac{4}{11}$ as a mixed state of CF's with two and four attached vortices (fluxes) is not very accurate in a sense that the two additional vortices (fluxes) attached to each spin-reversed CF are not vortices of the many-body wave function expressed in terms of the same coordinates (fluxes of the same effective magnetic field) as the original two attached to each electron (to form CF's). The correct interpretation necessarily involves reapplication of the CF transformation to some of the original CF's (those in a partially filled reversed-spin LL), in analogy to the CF hierarchy proposed

by Sitko *et al.* [89, 98] and essentially equivalent [120] to Haldane's hierarchy [36]. Let us stress that it is the short range of the QE_R–QE_R repulsion shown here that justifies application of Haldane hierarchy to QE_R's (or, equivalently, spin-reversed CF's).

Second, in analogy to the fractionally charged excitons (FCX's) [19, 123] consisting of a number of QE's of a spin-polarized 2DEG bound to a valence-band hole h, we discuss the possible formation and radiative recombination of similar complexes denoted as FCX_R's and containing one or more QE_R's bound to a hole. We find that different optical selection rules for FCX's and FCX_R's could allow optical detection of QE_R's in the 2DEG without need for direct polarization measurement.

The properties of spin-reversed quasielectrons (QE_R) are studied by exact numerical diagonalization in an ideal 2DEG with zero width and no disorder. The magnetic field B is assumed to be sufficiently large (the cyclotron energy $\hbar\omega_c \propto B$ much larger than the interaction energy scale $e^2/\lambda \propto \sqrt{B}$, where λ is the magnetic length) that only the lowest LL need be considered. In our studies we use the model discussed in detail in Chap. 3 and the electronic spin is included by adding a quantum number σ denoting the projection of spin. The many-electron interaction Hamiltonian H_{ee} (Eq. 3.23) is diagonalized in the basis of Slater determinants (Sec. 3.2), which allows automatic resolution of two good many-body quantum numbers, projection of spin ($S_z = \sum \sigma_i$) and angular momentum ($L_z = \sum m_i$). The other two, length of spin (S) and angular momentum (L), are resolved numerically in the diagonalization of each appropriate (S_z, L_z) Hilbert subspace.

In order to describe the reversed-spin fractionally charged exciton (FCX_R) states, a single valence-band hole h is added to the model N-electron system. Since, as for FCX's, the formation of FCX_R states requires weakening of the electron–hole attraction compared to the electron–electron repulsion [123], the hole is placed on a parallel plane, separated by a distance d (of the order of λ) from the 2DEG. Because the physics of an isolated FCX or FCX_R to a good approximation does not depend on the (possibly complicated) structure of the valence band, the single-hole wave functions are taken

the same as for electrons (except for the reversed signs of m and σ). This means that both inter-LL hole scattering and the mixing between heavy- and light-hole subbands are ignored. The weak electron–hole exchange is also neglected so that the hole spin has no effect on the dynamics of an FCX or $\mathrm{FCX_R}$, and the interaction of a hole with the 2DEG is described by the following spin-conserving term

$$H_{eh} = \sum c^{\dagger}_{m_1\sigma} h^{\dagger}_{m_2} h_{m_3} c_{m_4\sigma} \langle m_1 m_2 | V_{eh} | m_3 m_4 \rangle \tag{4.1}$$

in the total Hamiltonian $H = H_{ee} + H_{eh}$. The operators $h^{\dagger}_m$ and h_m create and annihilate a hole in the orbital $|m\rangle$ of the valence band, and the electron–hole interaction is defined by the Coulomb potential $V_{eh}(r) = -e^2/\sqrt{r^2+d^2}$. The exclusion of the hole–hole interaction effects from H reflects the fact that $\nu_h \ll \nu$. Interaction Hamiltonian H is diagonalized in the basis of single-particle configurations

$$|m_1\sigma_1 \ldots m_N\sigma_N; m_h\rangle = c^{\dagger}_{m_1\sigma_1} \ldots c^{\dagger}_{m_N\sigma_N} h^{\dagger}_{m_h} |\mathrm{vac}\rangle\,, \tag{4.2}$$

and the set of good quantum numbers labelling many-electron–one-hole eigenstates includes S_z and S of the electrons, hole spin σ_h (omitted in our equations), and the length (L) and projection (L_z) of angular momentum of the total electron–hole system.

4.2 Stability and Single Particle Properties of Spin-Reversed Quasielectrons

There are two types of elementary charge-neutral excitations of Laughlin $\nu = (2p+1)^{-1}$ ground states, carrying spin $K = 0$ or 1, respectively. Their dispersion curves (energy as a function of wave vector), $\mathcal{E}_K(k)$, have been studied for all combinations of p and K. While the formulae for the $\nu = 1$ ground state have been evaluated analytically [13, 35, 49], in Fig. 4.1 we present the exact numerical results for $\nu = \frac{1}{3}$ obtained from our exact diagonalization of up to $N = 11$ electrons on Haldane's sphere. As an example, in Fig. 4.1(a), we show the entire low-energy spectrum of an $N = 9$ system with all spins polarized and with one reversed spin (Hilbert subspaces of total spin

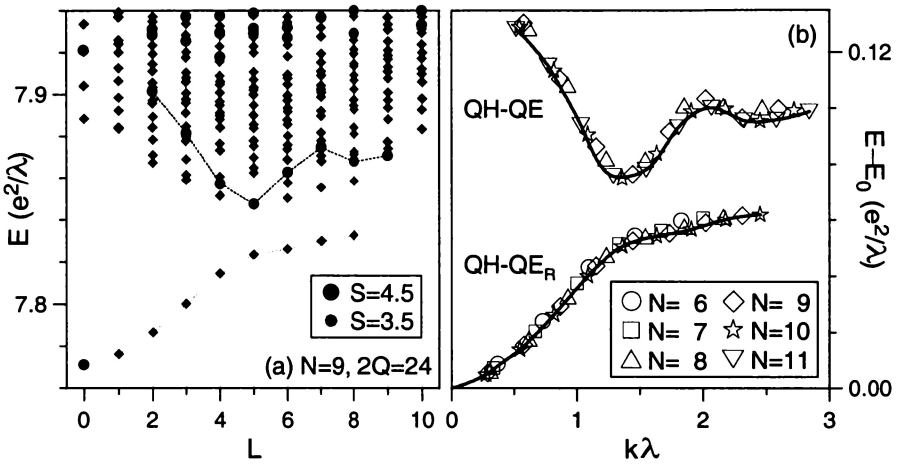


Figure 4.1: Elementary excitations of the $\nu = \frac{1}{3}$ Laughlin state. (a) The energy spectrum (Coulomb energy E versus angular momentum L) of the system of $N = 9$ electrons on Haldane sphere at the monopole strength $2Q = 3(N-1) = 24$. Black dots and grey diamonds mark states with the total spin $S = \frac{1}{2}N = \frac{9}{2}$ (maximum polarization) and $S = \frac{1}{2}N - 1 = \frac{7}{2}$ (one reversed spin), respectively. Ground state is the Laughlin $\nu = \frac{1}{3}$ state. Lines connect states containing one QE–QH ($S = \frac{9}{2}$) or $\mathrm{QE_R}$–QH ($S = \frac{7}{2}$) pair. (b) The dispersion curves (excitation energy $\mathcal{E}_K = E - E_0$ versus wave vector k) for the $K = 0$ charge-density wave (QE–QH pair) and the $K = 1$ spin-density wave ($\mathrm{QE_R}$–QH pair) in the Laughlin $\nu = \frac{1}{3}$ ground state, calculated in the systems of $N \leq 11$ electrons on Haldane sphere. λ is the magnetic length and K is the number of reversed spins relative to a ferromagnetic state [105]

$S = \frac{1}{2}N - K = \frac{9}{2}$ and $\frac{7}{2}$ for $K = 0$ and 1, respectively), from which the dispersion curves $\mathcal{E}_K(k)$ are obtained. The energy E is plotted as a function of angular momentum L, and $2Q = 3(N-1) = 24$ is the strength of the magnetic monopole inside Haldane's sphere corresponding to the LL degeneracy $g = 2Q + 1 = 25$ and the Laughlin filling factor $\nu = (N-1)/(g-1) = \frac{1}{3}$ (for the details on Haldane's spherical geometry see Sec. 3.1). The energy E does not include the Zeeman term E_Z, which scales differently than the plotted Coulomb energy with the magnetic field B. The excitation energies $\mathcal{E}_K = E - E_0$ (where E_0 is the Laughlin ground state energy) have been calculated for the states identified in the finite-size spectra as the $K = 0$ charge-density wave and the $K = 1$ spin-density wave. These states are marked with dotted lines in Fig. 4.1(a). The values of $\mathcal{E}_K$ obtained for different $N \leq 11$ have been plotted together in Fig. 4.1(b) as a function of the wave vector $k = L/R = (L/\sqrt{Q})\lambda^{-1}$. Clearly, using the appropriate units of λ^{-1} for wave vector and e^2/λ for excitation energy in Fig. 4.1(b) results in the quick convergence of the curves with increasing N, and allows accurate prediction of the dispersion curves in an infinite system, as marked with thick lines. The most significant features of these curves are: (i) the finite gap $\Delta_0 \approx 0.076\, e^2/\lambda$ and the magneto-roton minimum $k \approx 1.5\lambda^{-1}$ in $\mathcal{E}_0(k)$, and (ii) the vanishing of $\mathcal{E}_1(k)$ in the $k \to 0$ limit (for $E_Z = 0$).

The similar nature of the charge- and spin-waves in the $\nu = \frac{1}{3}$ state to those at $\nu = 1$ lies at the heart of the CF picture (Sec. 2.3), in which these excitations correspond to promoting one CF from a completely filled lowest ($n = 0$) spin-$\downarrow$ CF LL either to the first excited ($n = 1$) CF LL of the same spin ($\downarrow$) or to the same CF LL ($n = 0$) but with the reversed spin ($\uparrow$). The three constituent QP's of which the charge- and spin-waves are composed: a hole in the $n = 0$ spin-$\downarrow$ CF LL and particles in the $n = 1$ spin-$\downarrow$ and $n = 0$ spin-$\uparrow$ CF LL's, are analogous to those in the electron LL's from which the charge- and spin-waves at $\nu = 1$ are built.

Independently of the CF picture, one can define three types of QP's (elementary excitations) of the Laughlin $\nu = \frac{1}{3}$ fluid (compare Sec. 2.2). They are Laughlin quasi-

holes (QH's) and quasielectrons (QE's) and Rezayi spin-reversed quasielectrons ($\mathrm{QE_R}$). The excitations in Fig. 4.1 are more complex in a sense that they consist of a (neutral) pair of QH and either QE ($K = 0$) or $\mathrm{QE_R}$ ($K = 1$). Each of the QP's is characterized by such single-particle quantities as (fractional) electric charge ($\mathcal{Q}_{\mathrm{QH}} = +\frac{1}{3}e$ and $\mathcal{Q}_{\mathrm{QE}} = \mathcal{Q}_{\mathrm{QER}} = -\frac{1}{3}e$), energy $\varepsilon_{\mathrm{QP}}$, or degeneracy g_{QP} of the single-particle Hilbert space. On Haldane's sphere, the degeneracy g_{QP} is related to the angular momentum l_{QP} by $g_{\mathrm{QP}} = 2l_{\mathrm{QP}}+1$, with $l_{\mathrm{QH}} = l_{\mathrm{QER}} = Q^*$ and $l_{\mathrm{QE}} = Q^*-1$ and $2Q^* = 2Q-2(N-1)$ being the effective monopole strength in the CF model (Sec. 3.3).

The energies $\varepsilon_{\mathrm{QP}}$ to create an isolated QP of each type in the Laughlin ground state have been previously estimated in a number of ways. Here, we present our results of exact diagonalization calculation for $N \leq 11$ ($\varepsilon_{\mathrm{QE}}$ and $\varepsilon_{\mathrm{QH}}$) and $N \leq 10$ ($\varepsilon_{\mathrm{QER}}$). In Fig. 4.2(a) we show an example of the numerical energy spectrum for the system of $N = 9$ electrons, in which an isolated QE or $\mathrm{QE_R}$ occurs at $2Q = 3(N-1)-1 = 23$ in the subspace of $S = \frac{1}{2}N = \frac{9}{2}$ and $S = \frac{1}{2}N-1 = \frac{7}{2}$, respectively. Both of these states have been identified in Fig. 4.2(a). To estimate $\varepsilon_{\mathrm{QE}}$ and $\varepsilon_{\mathrm{QER}}$, we use the standard procedure [31, 38, 39, 119, 120] to take into account the finite-size effects (the dependence of λ on $2Q$, $Q\lambda^2 = R^2$), and express the energies E of Fig. 4.2(a) in the units of e^2/λ with λ appropriate for $\nu = \frac{1}{3}$, before subtracting from them the Laughlin ground state energy of Fig. 4.1(a). Plotting the results for different values of N in Fig. 4.2(b) as a function of N^{-1} allows the extrapolation to an infinite system, with the limiting values of $\varepsilon_{\mathrm{QE}} = 0.0664\,e^2/\lambda$ and $\varepsilon_{\mathrm{QER}} = 0.0383\,e^2/\lambda$ (with the difference $\varepsilon_{\mathrm{QE}} - \varepsilon_{\mathrm{QER}} = 0.0281\,e^2/\lambda$ in remarkable agreement with Rezayi's original estimate [91] based on his numerics for $N \leq 6$). For completeness, we have also plotted the QH energies, which extrapolate to $\varepsilon_{\mathrm{QH}} = 0.0185\,e^2/\lambda$. Note that to obtain the so-called "proper" QP energies in a finite system [31, 36, 119], $\tilde{\varepsilon}_{\mathrm{QP}}(N)$, the term $\mathcal{Q}^2_{\mathrm{QP}}/2R$ must be added to each value in Fig. 4.2(b). The linear extrapolation of $\tilde{\varepsilon}_{\mathrm{QP}}(N)$ to $N^{-1} \to 0$ gives $\tilde{\varepsilon}_{\mathrm{QE}} = 0.0737\,e^2/\lambda$, $\tilde{\varepsilon}_{\mathrm{QER}} = 0.0457\,e^2/\lambda$, and $\tilde{\varepsilon}_{\mathrm{QH}} = 0.0258\,e^2/\lambda$. The energies of spatially separated QE–QH and $\mathrm{QE_R}$–QH pairs (activation energies in transport experiments) are hence equal

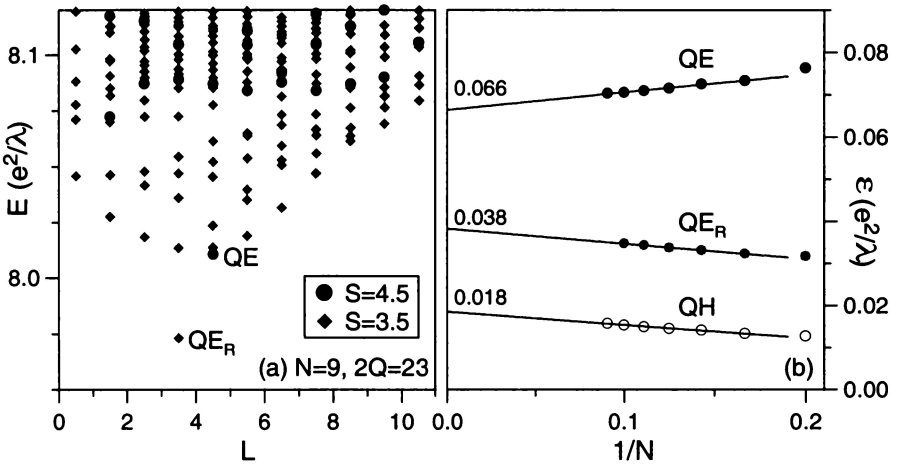


Figure 4.2: Quasiparticles in the $\nu = \frac{1}{3}$ Laughlin ground state. (a) The energy spectrum (Coulomb energy E versus angular momentum L) of the system of $N = 9$ electrons on Haldane sphere at the monopole strength $2Q = 3(N-1) - 1 = 23$. Black dots and grey diamonds mark states with the total spin $S = \frac{1}{2}N = \frac{9}{2}$ (maximum polarization) and $S = \frac{1}{2}N - 1 = \frac{7}{2}$ (one reversed spin), respectively. Ground state at $S = \frac{7}{2}$ is the reversed-spin quasielectron $\mathrm{QE_R}$ of the Laughlin $\nu = \frac{1}{3}$ fluid, and the lowest-energy state at $S = \frac{9}{2}$ is the Laughlin quasielectron QE. (b) The energies ε of all three types of quasiparticles of the $\nu = \frac{1}{3}$ state (QH, QE, and $\mathrm{QE_R}$) calculated in the systems of $N \leq 11$ electrons on Haldane sphere and plotted as a function of N^{-1}. The numbers give the results of linear extrapolation to an infinite (planar) system. λ is the magnetic length. [105]

to $\mathcal{E}_0(\infty) = \tilde{\varepsilon}_{\mathrm{QE}} + \tilde{\varepsilon}_{\mathrm{QH}} = 0.0995\, e^2/\lambda$ and $\mathcal{E}_1(\infty) = \tilde{\varepsilon}_{\mathrm{QER}} + \tilde{\varepsilon}_{\mathrm{QH}} = 0.0715\, e^2/\lambda$.

While the QH's are the only type of QP's that occur in low-energy states at $\nu < (2p+1)^{-1}$, the QE's and $\mathrm{QE_R}$'s are two competing excitations at $\nu > (2p+1)^{-1}$. As pointed out by Rezayi [91] and Chakraborty *et al.*, [15] whether QE's or $\mathrm{QE_R}$'s will occur at low energy depends on the relation between their energies including the Zeeman term, $\varepsilon_{\mathrm{QE}}$ and $\varepsilon_{\mathrm{QER}} + E_{\mathrm{Z}}$. Although it is difficult to accurately estimate the value of E_{Z} in an experimental sample because of its dependence on a number of factors (material parameters, well width w, density ϱ, magnetic field B, etc.), it seems that both scenarios with QE's and $\mathrm{QE_R}$'s being lowest-energy QP's are possible. For example, using the bulk value for the effective g^*-factor in GaAs ($dE_{\mathrm{Z}}/dB = 0.03$ meV/T) results in the $\mathrm{QE_R}$–QE crossing at $B = 18$ T, while including the dependence of g^* on w and B as described in Ref. [121] makes $\mathrm{QE_R}$ more stable than QE up to $B \sim 100$ T.

4.3 Interaction with Other Quasiparticles

Once it is established which of the QP's occur at low energy in a particular system (defined by ϱ, w, B, ν, etc.), their correlations can be understood by studying the appropriate pair interaction pseudopotentials [39, 89, 119, 124] (Sec. 2.4). On a plane, $\mathcal{R}$ for a pair of particles ab is the angular momentum associated with the (complex) relative coordinate, $z = z_a - z_b$. On Haldane's sphere, the compatible definition of $\mathcal{R}$ depends on the sign of $\mathcal{Q}_a\mathcal{Q}_b$ (compare Eq. 2.21): for a pair of opposite charges, $\mathcal{R}$ is the length of total pair angular momentum, $L = |\mathbf{l}_a + \mathbf{l}_b|$, while for two charges of the same sign, $\mathcal{R} = l_a + l_b - L$. In all cases, $\mathcal{R} \geq 0$ and larger $\mathcal{R}$ corresponds to a larger average ab separation [89, 119]. Furthermore, only odd values of $\mathcal{R}$ are allowed for indistinguishable ($a = b$) fermions.

Since the QE–QH and $\mathrm{QE_R}$–QH pseudopotentials have been plotted in Fig. 4.1 ($V_{\mathrm{QE-QH}} = \mathcal{E}_0$ and $V_{\mathrm{QER-QH}} = \mathcal{E}_1$), and the QE–QE and QH–QH pseudopotentials can be found for example in Ref. [120], we only need to discuss $V_{\mathrm{QER-QER}}$ and $V_{\mathrm{QE-QER}}$. Two $\mathrm{QE_R}$'s occur in an N-electron system with at least two reversed spins ($S \leq \frac{1}{2}N - 2$)

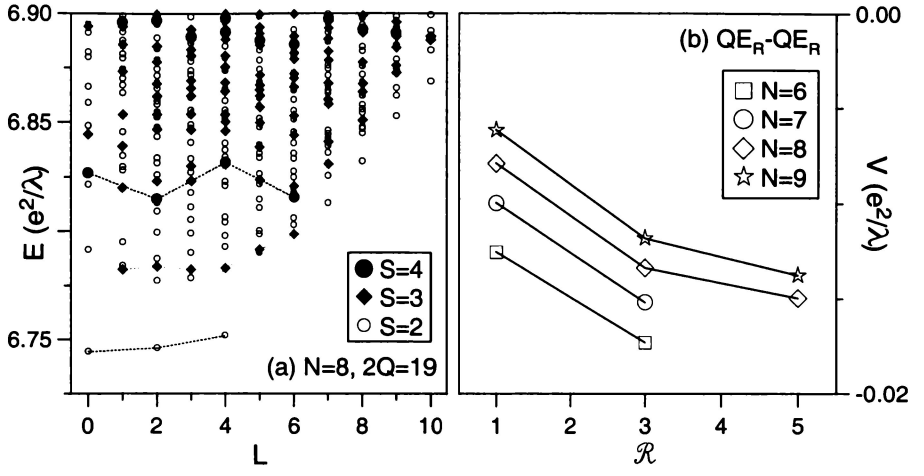


Figure 4.3: Interaction between two QE_R's. (a) The energy spectrum (Coulomb energy E versus angular momentum L) of the system of $N = 8$ electrons on Haldane sphere at the monopole strength $2Q = 3(N-1) - 2 = 19$. Black dots, grey diamonds, and open circles mark states with the total spin $S = \frac{1}{2}N = 4$ (maximum polarization), $S = \frac{1}{2}N - 1 = 3$ (one reversed spin), and $S = \frac{1}{2}N - 2 = 2$ (two reversed spins), respectively. Lines connect states containing one QE–QE ($S = 4$), QE–QE_R ($S = 3$), or QE_R–QE_R ($S = 2$) pair. (b) The pseudopotentials (pair energy V versus relative angular momentum $\mathcal{R}$) of the QE_R–QE_R interaction calculated in the systems of $N \leq 9$ electrons on Haldane sphere. λ is the magnetic length. [105]

and at $2Q = 3(N-1)-2$ (i.e., at $g = g_0 - 2$ where g_0 corresponds to the Laughlin state). An example of the energy spectrum is shown in Fig. 4.3(a) for $N = 8$ at $2Q = 19$. The lowest-energy states in the subspaces of $S = \frac{1}{2}N = 4$, $\frac{1}{2}N - 1 = 3$, and $\frac{1}{2}N - 2 = 2$ are connected with dashed lines and contain a QE–QE, QE–QE_R, and QE_R–QE_R pair, respectively. The angular momenta L that occur in these bands result from addition of l_{QE} and/or l_{QER} (with $l_{QE} = Q^* + 1 = \frac{7}{2}$ and $l_{QER} = Q^* = \frac{5}{2}$). For identical fermions, the addition must be followed by antisymmetrization that picks out only odd values of $\mathcal{R}$ for the QE–QE and QE_R–QE_R pairs.

An immediate conclusion from Fig. 4.3(a) is that the maximally spin-polarized ($S = \frac{1}{2}N$) system is unstable at the filling factor close but not equal to the Laughlin value of $\nu = \frac{1}{3}$ (the actual spin polarization decreases with decreasing E_Z, and $S = 0$ for

$E_Z = 0$). This was first pointed out by Rezayi [91] and interpreted in terms of an effective attraction between $K = 1$ spin-waves; here we prefer to use charged QP's as the most elementary excitations and explain the observed ordering of different S-bands by the fact that $\varepsilon_{QE} \neq \varepsilon_{QER}$ (at $E_Z = 0$, $\varepsilon_{QE} - \varepsilon_{QER} \approx 0.0281\, e^2/\lambda$) and the particular form of involved interaction pseudopotentials (see further in the text).

We have calculated the QE–QE_R and QE_R–QE_R pseudopotentials from the energy spectra as that in Fig. 4.3(a) by converting L into $\mathcal{R}$ and subtracting the Laughlin ground state energy and the energy of two appropriate QP's from the total N-electron energy, $V_{AB}(\mathcal{R}) = E(L) - E_0 - \varepsilon_A - \varepsilon_B$. To minimize the finite-size effects, all subtracted energies are given in the same units of e^2/λ_0, where $\lambda_0 = R/\sqrt{Q_0}$ corresponds to $2Q_0 = 3(N-1)$, i.e., to $\nu = \frac{1}{3}$. The result for $V_{QER-QER}$ and $N \leq 9$ is shown in Fig. 4.3(b). Clearly, obtained values of $V_{QER-QER}(\mathcal{R})$ still depend on N and, for example, the positive sign characteristic of repulsion between equally charged particles is only restored in the $N^{-1} \to 0$ limit with $V_{QER-QER}(1)$ of the order of $0.01\, e^2/\lambda$ (compare with discussion of the signs of V_{QE-QE} and V_{QH-QH} in Ref. [122]). However, it seems that the monotonic character of $V_{QER-QER}(\mathcal{R})$ is independent of N. More importantly, $V_{QER-QER}$ is also a super-linear function of $L(L+1)$. As discussed in Sec. 3.3, this implies [89, 119, 122] Laughlin correlations and incompressibility at $\nu_{QER} = (2p+1)^{-1}$, in analogy to the spin-polarized Laughlin states of QE's or QH's in Haldane's hierarchy picture [37, 120]. The most prominent of QE_R Laughlin states, $\nu_{QER} = \frac{1}{3}$, corresponds to the electronic filling factor of $\nu = \frac{4}{11}$ and the 75% spin polarization ($S = \frac{1}{4}N$). This state has been first suggested by Beran and Morf [7]. Since the $\nu_{QE} = \frac{1}{3}$ state is compressible [120], the experimental observation [104] of the FQHE at $\nu = \frac{4}{11}$ seems to prove the formation of QE_R's in the $\nu = \frac{1}{3}$ state without need for direct measurement of spin polarization. The expected critical dependence of the excitation gap at $\nu = \frac{4}{11}$ on the Zeeman gap E_Z might be revealed in tilted-field experiments. This dependence will be very different than at some other fractions. For example, the fact that incompressibility at $\nu = \frac{2}{5}$ can be a result of either maximally spin-polarized $\nu_{QE} = 1$ or completely

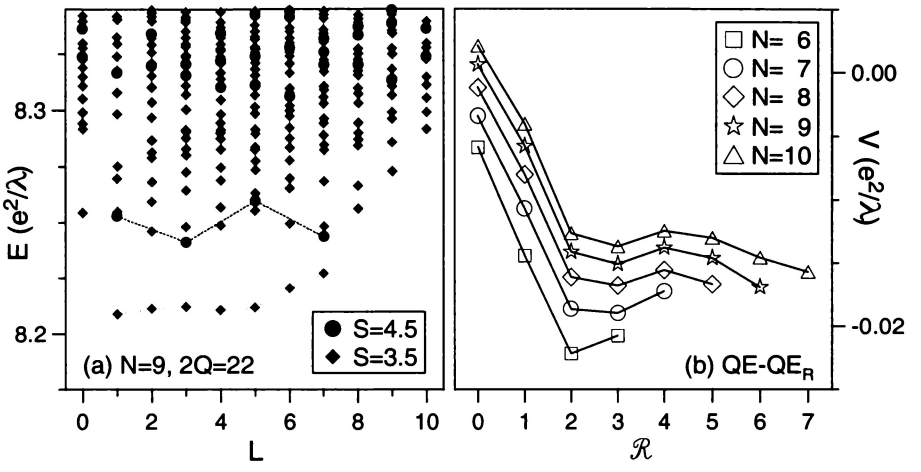


Figure 4.4: Interaction between QE and QE_R. (a) The energy spectrum (Coulomb energy E versus angular momentum L) of the system of $N = 9$ electrons on Haldane sphere at the monopole strength $2Q = 3(N-1) - 2 = 22$. Black dots and grey diamonds mark states with the total spin $S = \frac{1}{2}N = \frac{9}{2}$ (maximum polarization) and $S = \frac{1}{2}N - 1 = \frac{7}{2}$ (one reversed spin), respectively. Lines connect states containing one QE–QE ($S = \frac{9}{2}$) or QE–QE_R ($S = \frac{7}{2}$) pair. (b) The pseudopotentials (pair energy V versus relative angular momentum $\mathcal{R}$) of the QE–QE_R interaction calculated in the systems of $N \leq 10$ electrons on Haldane sphere. λ is the magnetic length. [105]

spin-unpolarized ($S = 0$) $\nu_{QER} = 1$ state gives rise to FQHE at this filling in both small and large E_Z regime. On the other hand, spin-unpolarized FQHE is not expected in the $\frac{1}{4} < \nu < \frac{1}{3}$ range (because spin-reversed QH's in the $\nu = \frac{1}{3}$ state do not exist), and the $\nu = \frac{2}{7}$ and $\frac{4}{13}$ states (corresponding [120] to $\nu_{QH} = \frac{1}{3}$ and $\frac{1}{5}$) should remain incompressible and compressible, respectively, over a wide range of E_Z.

The QE–QE_R pseudopotentials were calculated from similar spectra as that of $S = 3$ in Fig. 4.3(a). As another example, in Fig. 4.4(a) we show the spectrum for $N = 9$, in which only two values of $S = \frac{1}{2}N = \frac{9}{2}$ and $\frac{1}{2}N - 1 = \frac{7}{2}$ have been included. The lowest energy states in these two S-subspaces (connected with dashed lines) contain a QE–QE and QE–QE_R pair, respectively. Using the same procedure as for $V_{QER-QER}$, we have calculated $V_{QE-QER}(\mathcal{R})$. The results for $N \leq 10$ are presented in Fig. 4.4(b).

As for $V_{\mathrm{QER-QER}}$ in Fig. 4.3(b), the values of $V_{\mathrm{QE-QER}}(\mathcal{R})$ calculated in a finite system depend on N. The values extrapolated to the $N^{-1} \to 0$ limit are also similar, with $V_{\mathrm{QE-QER}}(0) \to 0.015\, e^2/\lambda$ and $V_{\mathrm{QE-QER}}(1) \to 0.01\, e^2/\lambda$.

Despite finite-size errors, the comparison of the curves for $N \leq 10$ is sufficient to notice quite different behavior of $V_{\mathrm{QE-QER}}(\mathcal{R})$ from both $V_{\mathrm{QER-QER}}(\mathcal{R})$ and $V_{\mathrm{QE-QE}}(\mathcal{R})$. Two important features of the $V_{\mathrm{QE-QER}}$ pseudopotential can be established: (i) the QE–$\mathrm{QE_R}$ repulsion is relatively strong at $\mathcal{R} \leq 1$ (short range) and saturates at larger $\mathcal{R}$, and (ii) $V_{\mathrm{QE-QER}}$ is super-linear in $L(L+1)$ only at $1 \leq \mathcal{R} \leq 3$, but sub-linear at $0 \leq \mathcal{R} \leq 2$ and at larger $\mathcal{R}$. As a consequence, the short-range criterion [89, 119, 124] (see Secs. 2.4 and 3.3) applied to $V_{\mathrm{QE-QER}}$ yields Laughlin correlations for QE–$\mathrm{QE_R}$ pairs only at $m = 2$. The term "Laughlin correlations" used here is defined in Sec. 3.3 as a tendency to avoid pair states with $\mathcal{R}$ smaller than certain m. At $\nu \leq m^{-1}$, these correlations are described by a Jastrow prefactor $\prod_{ij}(x_i - y_j)^m$ in the many-body wave function (Eq. 2.15), where x and y are complex QE and $\mathrm{QE_R}$ coordinates, respectively.

Although it is not clear if QE's and $\mathrm{QE_R}$'s could coexist in the $\nu = \frac{1}{3}$ "parent" state in an experimental system (such mixed state would be sensitive to the value of E_{Z}), one can ask if such two-component QE–$\mathrm{QE_R}$ plasma could also be incompressible. This question can be answered within the generalized CF model [89, 118] for all allowed combinations of Jastrow exponents $[m_{\mathrm{QE-QE}}, m_{\mathrm{QER-QER}}, m_{\mathrm{QE-QER}}]$. In this model, the reduced (effective) LL degeneracies of QP's are given by $g^*_{\mathrm{QE}} = g_{\mathrm{QE}} - (m_{\mathrm{QE-QE}} - 1)(N_{\mathrm{QE}} - 1) - m_{\mathrm{QE-QER}} N_{\mathrm{QER}}$ and $g^*_{\mathrm{QER}} = g_{\mathrm{QER}} - (m_{\mathrm{QER-QER}} - 1)(N_{\mathrm{QER}} - 1) - m_{\mathrm{QE-QER}} N_{\mathrm{QE}}$, and the incompressibility condition is $N_{\mathrm{QP}} = g^*_{\mathrm{QP}}$ for both QE's and $\mathrm{QE_R}$'s. In the above, g is the LL degeneracy of electrons and N_{QP} denotes the number of QP's of each type. It turns out that because the three involved QP pseudopotentials are not generally super-linear in $L(L+1)$, only few combinations of exponents $[m_{\mathrm{QE-QE}}, m_{\mathrm{QER-QER}}, m_{\mathrm{QE-QER}}]$ are allowed, and of those only [1,1,2] satisfies the incompressibility condition. The hypothetical [1,1,2] state of the QE–$\mathrm{QE_R}$ fluid corresponds to $\nu = \frac{5}{13}$ and 80% polarization ($S = \frac{3}{10}N$). Finite realizations of this state on Haldane's sphere occur for $N = 5q + 4$

($q \geq 1$) at $2Q = 13q + 7$, and have $N_{\rm QE} = q$ and $N_{\rm QER} = q + 2$, which yields $S = \frac{3}{2}q$.

4.4 Optical Properties

Once the single-particle energies ε and the two-particle interaction pseudopotentials $V(\mathcal{R})$ of all three types of QP's have been calculated, let us now turn to their optical properties. The effect of QE's on the photoluminescence (PL) spectrum of the Laughlin fluid has been studied in great detail [89, 123]. The crucial facts are: (i) The PL spectrum can be understood in terms of QE's and their interaction with one another and with a valence-band hole (h) only in the "weak-coupling regime" in which the electron–electron repulsion is sufficiently weak compared to the electron–hole attraction; this is realized in "asymmetric" structures in which the electron and hole layers are separated by a finite distance d (of the order of λ). (ii) In this regime, a positively charged h can bind one or two QE's to form "fractionally charged excitons" (FCX), hQE or hQE$_2$. (iii) The 2D translational invariance results in orbital selection rules for the radiative recombination of FCX's; it turns out that the only bright states are hQE* (an excited state of the dark hQE) and hQE$_2$.

In analogy, we expect that a valence hole h could also form bound states with one or more QE$_{\rm R}$'s, denoted by FCX$_{\rm R}$. However, unlike for FCX's, the stability of FCX$_{\rm R}$ complexes should depend on the Zeeman energy, the binding of more than one QE$_{\rm R}$ should be more difficult due to the stronger QE$_{\rm R}$–QE$_{\rm R}$ repulsion, different angular momenta of QE and QE$_{\rm R}$ should result in different optical selection rules of FCX$_{\rm R}$, and the possible annihilation of a hole with a reversed-spin electron should cause different polarization of FCX$_{\rm R}$ emission. To study the possible binding of FCX$_{\rm R}$'s we begin with the h–QE$_{\rm R}$ pseudopotential, shown in Fig. 4.5(a) for a $7e$–h system in which a hole interacts with $N = 7$ electrons and for a few different values of d/λ. The values of $2Q = 3(N-1) - 1 = 17$ and $S = \frac{1}{2}N - 1 = \frac{5}{2}$ are chosen so that one QE$_{\rm R}$ is present in the Laughlin $\nu = \frac{1}{3}$ state and interacts with the hole. In the CF picture of this configuration, $2Q^* = 2Q - 2(N-1) = 5$ so that six CF's fill completely the lowest

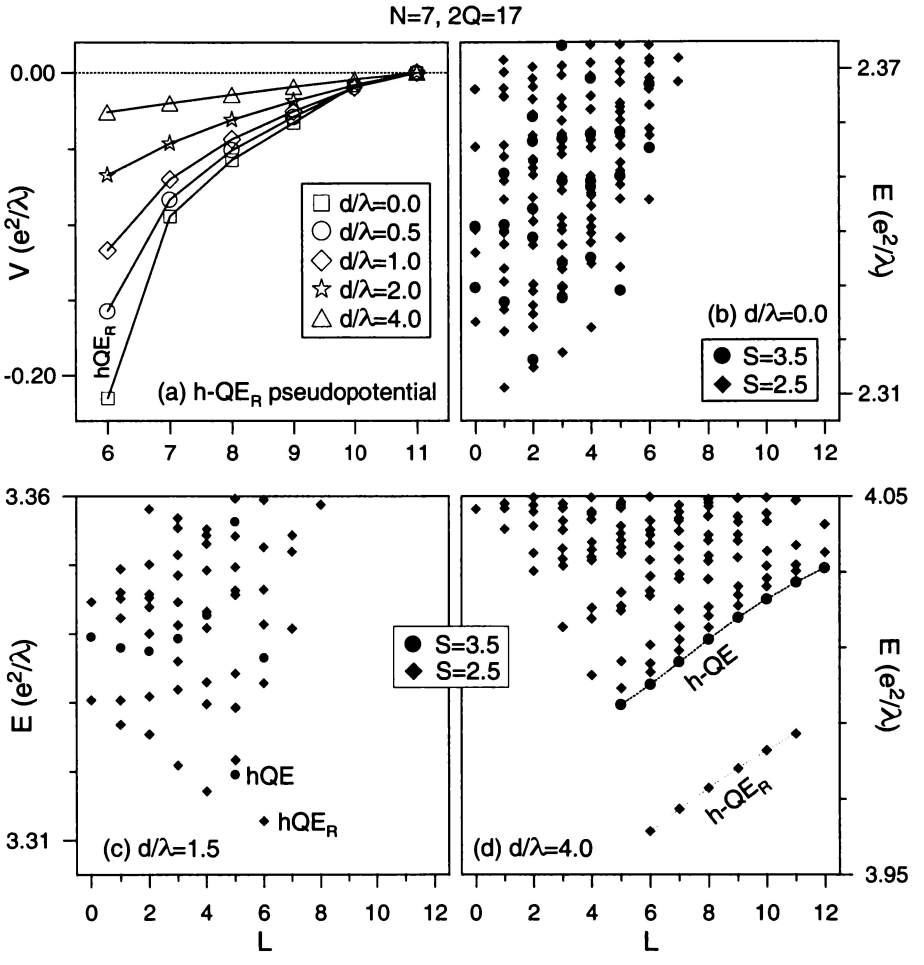


Figure 4.5: Interaction between quasiparticles and a valence band hole. (a) The pseudopotentials (pair energy V versus pair angular momentum L) of the h–$\mathrm{QE_R}$ interaction calculated in the system of $N = 7$ electrons and one valence hole (h) on Haldane sphere at the monopole strength $2Q = 3(N-1)-1 = 17$. Different symbols correspond to different separations d between the electron and hole planes. (bcd) The energy spectra (Coulomb energy E versus angular momentum L) of the same, seven-electron–one-hole system at $2Q = 17$ at three different values of d. Black dots and grey diamonds mark states with the total electron spin $S = \frac{1}{2}N = \frac{7}{2}$ (maximum polarization) and $S = \frac{1}{2}N - 1 = \frac{5}{2}$ (one reversed spin), respectively. Lines in (d) connect states containing one h–QE ($S = \frac{7}{2}$) or h–$\mathrm{QE_R}$ ($S = \frac{5}{2}$) pair. The lowest-energy $S = \frac{7}{2}$ and $\frac{5}{2}$ states in (c) are the fractionally charged excitons, hQE and $h\mathrm{QE_R}$, respectively. λ is the magnetic length. [105]

CF LL of $g^* = 2Q^* + 1$, leaving the seventh CF in the reversed-spin LL. The filled LL is incompressible, and only the single reversed-spin CF (i.e., $\mathrm{QE_R}$) correlates with the hole. The $V_{h-\mathrm{QER}}$ is plotted as a function of the pair angular momentum whose values ($6 \leq L \leq 11$) result from addition of $l_h = Q$ and $l_{\mathrm{QER}} = Q^*$. To ensure that exactly one $\mathrm{QE_R}$ is present in the Laughlin fluid and interacts with the hole at an arbitrary (small) value of d, a special procedure [123] has been used in which the electric charge of the hole is reduced to $e/\epsilon \ll e$. Clearly, the decrease of $V_{h-\mathrm{QER}}$ with a decrease of L (average h–$\mathrm{QE_R}$ separation) indicates h–$\mathrm{QE_R}$ attraction. The strength of this attraction, that is the binding energy $\Delta_{h\mathrm{QER}} \sim |V_{h-\mathrm{QER}}(l_h - l_{\mathrm{QER}})|$, depends on d and is similar to $\Delta_{h\mathrm{QE}}$; compare with Ref. [123]. Therefore, in analogy to the QE case, we expect that bound $h\mathrm{QE_R}$ states will occur in a system containing free $\mathrm{QE_R}$'s at the values of d at which $\Delta_{h\mathrm{QE}}$ and $\Delta_{h\mathrm{QER}}$ is smaller than the Laughlin gap to create additional QE–QH pairs (note that since the projection S_z of the total electron spin is conserved at any d, FCX or $\mathrm{FCX_R}$ does not couple to virtual $\mathrm{QE_R}$–QH excitations).

In order to verify the above hypothesis, we have calculated the $7e$–h energy spectra with up to one reversed spin ($S = \frac{1}{2}N = \frac{7}{2}$ and $S = \frac{1}{2}N - 1 = \frac{5}{2}$). The results for $d/\lambda = 0$, 1.5, and 4 are presented in Fig. 4.5(bcd). As expected, the $h\mathrm{QE_R}$ ground state develops together with the spin-polarized hQE state at d larger than about λ. The energy difference between $h\mathrm{QE_R}$ and hQE states at $d/\lambda = 1.5$ is only about $0.007\ e^2/\lambda$, which is small compared to $\varepsilon_{\mathrm{QE}} - \varepsilon_{\mathrm{QER}}$. This is because hQE couples stronger than $h\mathrm{QE_R}$ to virtual QE–QH pair excitations of the underlying Laughlin state (QE–$\mathrm{QE_R}$ repulsion at short range is stronger than QE–QE repulsion). At d much larger than λ, the lowest energy states in Fig. 4.5(d) contain well defined h–QE or h–$\mathrm{QE_R}$ pairs with all possible values of L. The coupling to the virtual QE–QH excitations is reduced, and the h–$\mathrm{QE_R}$ and h–QE bands are separated by about the single-particle gap $\varepsilon_{\mathrm{QE}} - \varepsilon_{\mathrm{QER}}$.

To compare the optical properties of hQE and $h\mathrm{QE_R}$, it is essential to notice that, because $l_{\mathrm{QER}} \neq l_{\mathrm{QE}}$, also $l_{h\mathrm{QER}} = l_h - l_{\mathrm{QER}} = N - 1$ is different from $l_{h\mathrm{QE}} = l_h - l_{\mathrm{QE}} = N - 2$. The orbital selection rule for radiative recombination of bound FCX or $\mathrm{FCX_R}$

states results from the fact that an annihilated, optically active electron–hole pair carries no angular momentum [4, 27, 121, 123]. Therefore, the angular momenta of the initial (bound) state and a final state in the emission process must be equal. On the other hand, it is known [19, 123] that only those emission processes with minimum number of QP's involved can have significant spatial overlap with an initial (bound) state of small size, and thus significant intensity (oscillator strength τ^{-1}). Thus, hQE or $h\mathrm{QE_R}$ must both recombine to leave two QH's in the final state (and no additional QE–QH or $\mathrm{QE_R}$–QH pairs). The allowed angular momenta of two identical QH's [in the final, $(N-1)e$ system] each with $l_{\mathrm{QH}} = \frac{1}{2}N$ are $L_{2\mathrm{QH}} = N - \mathcal{R}_{\mathrm{QH}}$, where $\mathcal{R}_{\mathrm{QH}}$ is an odd integer. The comparison of $L_{2\mathrm{QH}}$ with $l_{h\mathrm{QE}}$ and $l_{h\mathrm{QER}}$ makes it clear that, in contrast to the dark hQE, the $h\mathrm{QE_R}$ ground state is radiative. Since $h\mathrm{QE_R}$ is the simplest of all $\mathrm{FCX_R}$'s and bright at the same time, its emission is expected to dominate the PL spectrum of a Laughlin fluid at $\nu > \frac{1}{3}$, in which free $\mathrm{QE_R}$'s are present. The larger $\mathrm{FCX_R}$ complexes, $h(\mathrm{QE_R})_2$ and $h\mathrm{QE_RQE}$ are also found in the numerical calculation at $d > \lambda$ (see Fig. 4.6), but being less strongly bound (due to larger $\mathrm{QE_R}$–$\mathrm{QE_R}$ and $\mathrm{QE_R}$–QE repulsion at short range) they are not expected to form as easily as $h\mathrm{QE_2}$ does in a spin-polarized system. Moreover, $h(\mathrm{QE_R})_2$ turns out dark, and the formation of $h\mathrm{QE_RQE}$ requires the presence of both QE's and $\mathrm{QE_R}$'s in the unperturbed electron system, which further limits the contribution of these bound states to the PL spectrum. Let also add that since $h\mathrm{QE_R}$ emits by recombination of a valence hole with $\frac{1}{3}$ of an electron with reversed spin ($\mathrm{QE_R}$ in the initial state) and $\frac{2}{3}$ of an electron with majority spin (two QH's in the final state), the emitted photon should be only partially polarized. This is in contrast to a completely polarized emission of the bright FCX complexes, hQE* and $h\mathrm{QE_2}$. Therefore, the partially unpolarized emission in the "weak-coupling" regime ($d > \lambda$) could be an indication of the presence of $\mathrm{QE_R}$'s in the electron fluid.

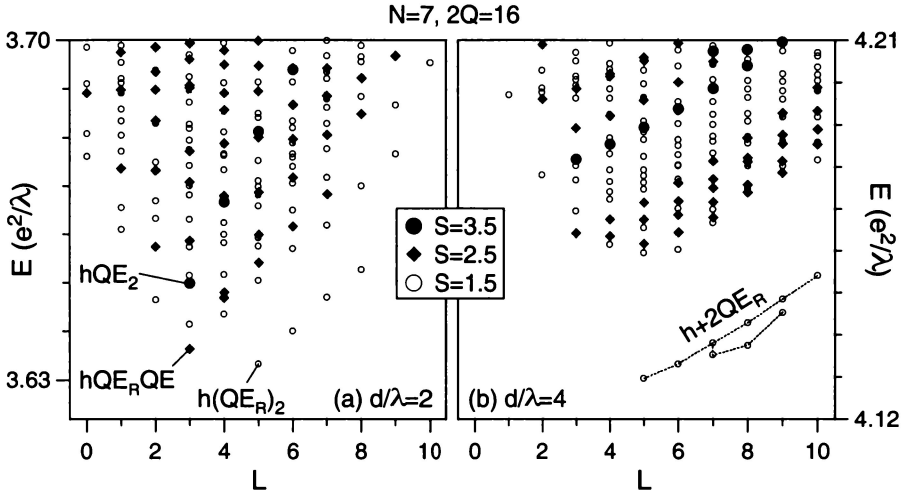


Figure 4.6: The energy spectra (Coulomb energy E versus angular momentum L) of the system of $N = 7$ electrons and one valence hole (h) on Haldane sphere at the monopole strength $2Q = 3(N-1) - 2 = 16$, at the separations $d = 2\lambda$ (a) and 4λ (b) between the electron and hole planes. Black dots, grey diamonds, and open circles mark states with the total electron spin $S = \frac{1}{2}N = \frac{7}{2}$ (maximum polarization), $S = \frac{1}{2}N - 1 = \frac{5}{2}$ (one reversed spin), and $S = \frac{1}{2}N - 2 = \frac{3}{2}$ (two reversed spins), respectively. The lowest-energy $S = \frac{7}{2}$, $\frac{5}{2}$, and $\frac{3}{2}$ states in (a) are the fractionally charged excitons, $h\mathrm{QE}_2$, $h\mathrm{QE_RQE}$, and $h(\mathrm{QE_R})_2$, respectively. The lowest-energy band of $S = \frac{3}{2}$ states marked with lines in (b) contains all possible states of two $\mathrm{QE_R}$'s and one h. λ is the magnetic length. [105]

Chapter 5

Spin Flip Excitations and Skyrmions

The spin excitations at $\nu = 1$ have been widely studied both theoretically [11, 32, 69, 78, 102, 129] and experimentally [2, 5, 54, 73, 75, 95, 110] in an extended 2DEG as well as in finite-size quantum Hall droplets [81, 82, 114]. It is therefore known that even in the absence of the Zeeman energy (E_Z) the $\nu = 1$ GS is ferromagnetic and translationally invariant (hence non-degenerate). The only excitations beyond the cyclotron gap $\hbar\omega_c$ are the *spin waves* (SW) with the number of reversed spins (relative to ferromagnetic state) $K = 1$ and the angular momentum $L = 1, 2, 3, \ldots$. A single SW (called also a spin-exciton) consists of a vacancy (hole) in the spin-$\downarrow$ level bound to an electron in the spin-$\uparrow$ level. Its dispersion curve is given by [49] $E_{SW}(k) = E_0 + E_Z + E_C\sqrt{\pi/2}[1 - \exp(-\kappa^2)I_0(\kappa^2)]$, where E_0 is the $\nu = 1$ GS energy, $E_C = e^2/\lambda$, $k = \frac{L}{\lambda\sqrt{Q}}$ is a longitudinal wave vector, $\kappa = k\lambda/2$ and I_0 is the modified Bessel function. It has been shown [125] that the SW's each with $L = 1$ condense into an ordered (with parallel angular momenta), correlated and noninteracting state. The interaction energy of this condensate is linear in spin polarization, which gives rise to a gapless and continuous density of states.

Interestingly, adding an extra particle (a reversed-spin electron or a hole) to the

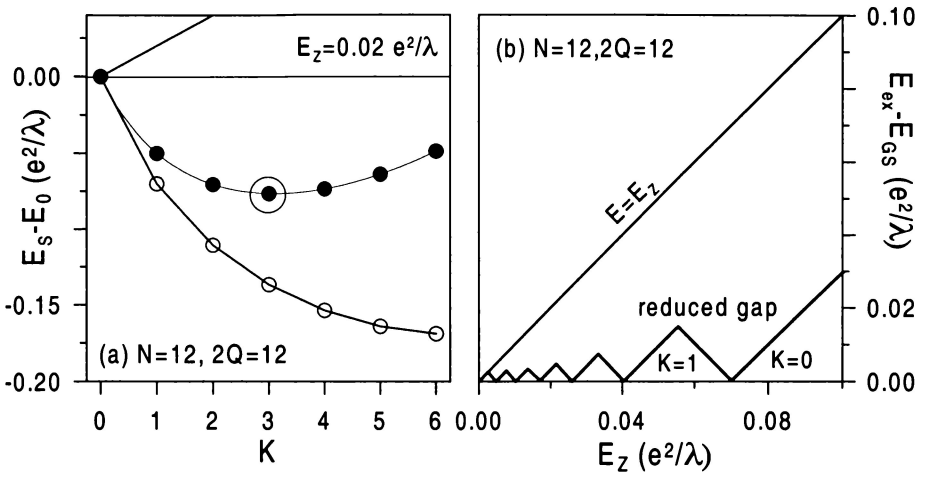


Figure 5.1: A finite system of $N = 12$ electrons at $2Q = 12$ ($\nu = 1^{\pm}$). (a) The excitation energy from the ferromagnetic GS E_0 to a skyrmionic state E_S vs the topological charge of the skyrmion K (number of SW's created in a system); open symbols: in the absence of the Zeeman energy; solid dots: adding the Zeeman energy E_Z causes transition to the GS with $K = 3$ (circled). (b) The reduced energy gap between the skyrmionic GS $E_{GS}(K)$ and the first excited state E_{ex} as a function of the Zeeman energy E_Z. The $E = E_Z$ function is the corresponding energy gap at precisely $\nu = 1$. [107]

$\nu = 1$ ferromagnetic GS will cause the formation of *skyrmions* or *anti-skyrmions* $S_K^{\pm}$ [66, 99, 102, 129], particle-like charged excitations with large spin. In Fig. 5.1(a-b) we illustrate it on the example of $N = 12$ electrons on Haldane sphere at $2Q = 12$, which due to the particle-hole symmetry can be interpreted as either an extra or missing electron in the $\nu = 1$ GS of 13 electrons, and will be denoted here as $\nu = 1^{\pm}$. In the absence of Zeeman energy, the $K = 0$ GS may become unstable [33] (open symbols in Fig. 5.1(a)). Depending on the value of Zeeman energy (controlled e.g. by hydrostatic pressure [43, 101]) the skyrmionic state with appropriate K will become the GS of the system. The skyrmionic spin excitation gap will be significantly reduced compared to E_Z (see Fig. 5.1(b)). Importantly, due to an exact mapping between the unpolarized electron ($\uparrow$–$\downarrow$) and polarized electron–valence-hole (e–h) systems in the lowest LL [71], the S_K states are equivalent to the charged multi-excitons [83, 113] ($X_K^{\pm}$) consisting of K

neutral excitons bound to an extra e or h (see Sec. 4.1). This allows cross-interpretation of studies of spin and optical excitations.

Whether the insertion of an additional reversed-spin particle (from the edge) into a bulk of the droplet will cause its complete depolarization (in the absence of E_Z), depends on the details of the interaction pseudopotential. Wójs and Quinn [125] found a general criterion that allows prediction of the presence or absence of skyrmions in a system of spin-$\frac{1}{2}$ particles half-filling a spin-degenerate shell. According to this criterion, the skyrmion states will be the eigenstates of the system with lowest energies, and these energies will decrease with increasing the topological charge K, if and only if the electron-electron interaction pseudopotential $V_{ee}(\mathcal{R})$ (see Sec. 2.4): (i) is not only repulsive, but also superharmonic (Sec. 3.3) at $\mathcal{R} = 0$, (ii) decreases sufficiently quickly with increasing $\mathcal{R}$ between $\mathcal{R} = 1$ and 3, $\mathcal{R} = 3$ and 5, etc.

Recent NMR experiments [24, 57] on the spin polarization at $\nu = \frac{1}{3}$ clearly indicate that skyrmions are more important near this filling factor than expected from previous theory [51]. Near $\nu = (2p + 1)^{-1}$ (p is an integer) Laughlin correlations [62] allow mapping [42, 47, 67] of the low-energy interacting-electron states onto the noninteracting composite fermion (CF) states with an effective filling factor $\nu^* \approx 1$ (Sec. 2.3). The Chern-Simons transformation, in which $2p$ magnetic flux quanta are attached to each electron, results in the effective CF LL degeneracy of $g^* = g - 2p(N - 1)$. On a sphere [89], this replaces the electronic $2l = 2Q \approx (2p + 1)(N - 1)$ by $2l^* = 2Q^* \approx N - 1$ (Sec. 3.3). As discussed in Sec. 4.2, analogously to the case of charge and spin waves at $\nu = 1$, those at $\nu = \frac{1}{3}$ are composed of three elementary QP's: a hole in the $n = 0$ spin-$\downarrow$ CF LL and particles in the $n = 1$ spin-$\downarrow$ and $n = 0$ spin-$\uparrow$ CF LL's. The three types of QP's of the Laughlin $\nu = \frac{1}{3}$ fluid can be defined independently of the CF picture: Laughlin quasiholes (QH's) and quasielectrons (QE's) and Rezayi spin-reversed quasielectrons ($\mathrm{QE_R}$'s) [91, 105]. The formation of small skyrmions and anti-skyrmions near $\nu = \frac{1}{3}$ was confirmed in both, experiments [53, 65] and in numerical calculation [70]. The criterion for the occurrence of skyrmions in a $\nu = \frac{1}{3}$ fluid, which is an example

of a system with borken particle(↑)–hole(↓) symmetry, is similar to the one at $\nu = 1$ with the exception that the condition (ii) must be rephrased in terms of the particle-hole pseudopotential V_{eh} which must increase monotonically as a function of a wave vector k [125].

Chapter 6

Hyperfine Coupling of Quantum Hall States to Nuclear Spins

6.1 Introduction

One of the most promising scenarios for implementation of a quantum computer is to manipulate nuclear spin in heterojunctions via hyperfine interaction with the electron spins under the conditions of quantum Hall effect. This idea was motivated by the optically pumped NMR measurments [5, 110] on GaAs quantum well structures of a dramatic enhancement of the very small nuclear relaxation rate which characterizes the QH ferromagnetic $\nu = 1$ GS, and of a sharp decrease of the Knight shift, when the filling factor was moved away from $\nu = 1$. Similar effects were observed [24] near $\nu = \frac{1}{3}$.

The overview of earlier work done on nuclear relaxation processes can be found in Chap. 1. Here, we report on detailed numerical studies of the coupling between the incompressible $\nu = 1$ and $\frac{1}{3}$ quantum Hall states and the localized nuclear spins. Following earlier discussion [74] we assume that the nuclear relaxation time is governed only by the hyperfine interaction with the electron spins. We find that the perturbation of the $\nu = 1$ or $\frac{1}{3}$ state by the hyperfine interaction with a localized spin results in the creation of a spin wave (SW) with a finite wave vector k and an energy $E(k)$ that is

larger than the electronic Zeeman gap, $E(k) \geq E(0) = E_Z$. A spectral function for this process is calculated and shown to vanish at both $k = 0$ and $k \to \infty$. The maximum of the spectral function is at $k \sim 1/\lambda$, i.e. at the energy larger than $E(0) = E_Z$ by a term of the order of $E_C = e^2/\lambda$, and the nuclear Zeeman energy is much smaller than both E_C and E_Z. Therefore the energy conservation law prevents flipping nuclear spins at (locally) $\nu = 1$ or $\frac{1}{3}$, even if E_Z was made arbitrarily small. This explains long relaxation times observed in experiments.

At ν slightly different from 1 or $\frac{1}{3}$, the spin excitations coupled to a localized spin are the "internal excitations" of skyrmions in which their number of reversed spins K and angular momentum of a skyrmion change by one [33, 69, 125]. Remarkably, we find that the oscillator strength for this process increases with the skyrmion size K. Since the energy of the $K \to K + 1$ excitation is much smaller than E_Z (and, in particular, it can be made equal to the nuclear Zeeman gap at the appropriate value of E_Z), it means that the skyrmion-nucleus spin-flip processes will be allowed by the energy conservation law. This explains the shortened relaxation times of nuclear spin states at ν slightly different from 1 or $\frac{1}{3}$.

At this stage of our study, we limit ourselves to the investigation of the mechanisms responsible for nuclear spin relaxation. We do not attempt to analyze the statistical mechanics of the relaxation rate of any non-equilibrium nuclear spin distribution, which will be the subject of our future study. The results discussed here will be published in Ref. [107].

6.2 Model

Following the earlier work on the spin excitations of the 2DEG in the quantum Hall regime [57, 53, 102, 125, 129] (Chap. 5), we study the coupling of these excitations to localized (e.g. nuclear) spins. The model to describe the 2DEG is that of Sec. 3.1, except that it is now extended to include the presence of a nucleus. The electrons are confined to a Haldane sphere [36] of radius R. The single-electron states (monopole

harmonics, see Eqs. 3.10 and 3.15) are the eigenstates [31, 36, 126] of magnitude (l) and projection (m) of angular momentum and of spin projection σ, and they form g-fold ($g = 2l + 1$) degenerate LL's labeled by $n = l - Q$.

The cyclotron energy $\hbar\omega_c \propto B$ is assumed much larger than the Coulomb energy $E_C = e^2/\lambda \propto \sqrt{B}$. However, no assumption is made about the electron Zeeman energy, and $\eta = E_Z/E_C$ is a (small) free parameter of the model. As a result, only the $\sigma = \downarrow$ and $\uparrow$ states of the lowest ($n = 0$) LL need be included in the calculation, denoted simply by $|m\sigma\rangle$.

The many-electron Hamiltonian in the lowest LL can be written as (compare Eq. 3.23)

$$\begin{aligned} H &= \sum c^\dagger_{m_1\sigma} c^\dagger_{m_2\sigma'} c_{m_3\sigma'} c_{m_4\sigma} \langle m_1 m_2 | V | m_3 m_4 \rangle \\ &+ \sum c^\dagger_{m\uparrow} c_{m\uparrow} E_Z, \end{aligned} \tag{6.1}$$

where $c^\dagger_{m\sigma}$ and $c_{m\sigma}$ are the electron creation and annihilation operators, the summation goes over all orbital and spin indices, and V is the Coulomb interaction potential. The many-electron states are expanded in the basis of Slater determinants

$$|m_1\sigma_1 \ldots m_N\sigma_N\rangle = c^\dagger_{m_1\sigma_1} \ldots c^\dagger_{m_N\sigma_N} |\text{vac}\rangle , \tag{6.2}$$

where $|\text{vac}\rangle$ stands for the vacuum state.

To study the relaxation processes of nuclear spins, we assume that the separation between nuclei is large so that their direct magnetic dipolar interaction can be neglected [74]. Also the temperature is assumed to be smaller than any relevant electronic energy scale and therefore the effects of electron scattering by the impurity potential need not be included. In such systems the nuclear relaxation time τ is governed only by the hyperfine interaction with the electron spins described by the contact interaction Hamiltonian [100]

$$\begin{aligned} F &= A \sum_{j,k} \mathbf{I_k S_j}\, \delta(\mathbf{r_j} - \mathbf{R_k}) \\ &= A \sum_{j,k} I_{kz} S_{jz} \delta(\mathbf{r_j} - \mathbf{R_k}) + \frac{1}{2} A \sum_{jk} \left[I_k^+ S_j^- + I_k^- S_j^+ \right] \delta(\mathbf{r_j} - \mathbf{R_k}), \end{aligned} \tag{6.3}$$

where A is the hyperfine coupling constant, $\mathbf{S_j}$ ($\mathbf{I_k}$) and $\mathbf{r_j}$ ($\mathbf{R_k}$) denote the spin and position of the jth electron (kth nucleus). The longitudinal part of F does not change the spin projection on the $\mathbf{B}$ direction, and therefore in our problem only the transverse part of F (the last term in Eq. 6.3) need be considered.

Let $|i\rangle_e$, $|i\rangle_n$, $|f\rangle_e$, and $|f\rangle_n$ stand for the initial and final many-body states of electrons and a nucleus, respectively. Electrons are weakly interacting with the nucleus, hence $|i\rangle = |i\rangle_e |i\rangle_n$ and

$$\langle f| A\sum_j S_j^+(r)I^-(R)\delta(r-R)\,|i\rangle = {}_n\langle f|\, I^-(R)\,|i\rangle_n\ {}_e\langle f|\, A\sum_j S_j^+(r)\delta(r-R)\,|i\rangle_e\,. \quad (6.4)$$

Here, we will not specify the nuclear states and will focus on the electronic contribution described by the last matrix element in the Eq. 6.4.

Due to the translational/rotational invariance of the 2DEG, the position of the nucleus can be conveniently chosen at the north pole of the sphere, where all electron wave functions (of the lowest LL) vanish, except for $|m=l,\uparrow\rangle$ and $|m=l,\downarrow\rangle$. On the Haldane sphere

$$\delta(r-R) = A'\delta(\hat{\Omega}-\hat{N}), \quad (6.5)$$

where $\hat{\Omega}$ is a position versor in spherical coordinates (Eq. 3.4), $\hat{N}$ stands for the north pole of the sphere (Sec. 3.1) and A' is a constant such that

$$\int A'\delta(\hat{\Omega}-\hat{N})\mathrm{d}\Omega = 1. \quad (6.6)$$

In the basis of Slater determinants, the electronic matrix element in Eq. 6.4 reads

$$\begin{aligned}
\langle m_1'\sigma_1'\ldots|\ F\ |m_1\sigma_1\ldots\rangle &= \left\langle m_1'\sigma_1',\ldots \middle| AA'\sum_j S_j^+\delta(\hat{\Omega}-\hat{N}) \middle| m_1\sigma_1\ldots \right\rangle = \\
&= \sum_{mm'} \left\langle m_1'\sigma_1'\ldots \middle| AA' c_{m'\uparrow}^+ c_{m\downarrow}\delta(\hat{\Omega}-\hat{N}) \middle| m_1\sigma_1\ldots \right\rangle = \\
&= \sum_{mm'} AA' \prod_{i\,(m_i\neq m)} \delta_{m_i m_i'}\delta_{\sigma_i\sigma_i'} \left\langle m'\sigma' \middle| c_{m'\uparrow}^+ c_{m\downarrow}\delta(\hat{\Omega}-\hat{N}) \middle| m\sigma \right\rangle = \\
&= \sum_{mm'} AA' \prod_{i\,(m_i\neq m)} \delta_{m_i m_i'}\delta_{\sigma_i\sigma_i'} \left\langle m' \middle| \delta(\hat{\Omega}-\hat{N}) \middle| m \right\rangle \left\langle \sigma' \middle| c_{m'\uparrow}^+ c_{m\downarrow} \middle| \sigma \right\rangle \quad (6.7)
\end{aligned}$$

where we applied the relation $S_j^+ = \sum_{mm'} c^+_{m'\uparrow} c_{m\downarrow}$. From the properties of monopole harmonics (Eqs. 3.15–3.17), one can evaluate explicitly

$$\begin{aligned}
&\left\langle m' \left| \delta(\hat{\Omega} - \hat{N}) \right| m \right\rangle = \\
&= \int \mathrm{d}\Omega \, Y^*_{Q,0,m}(\hat{\Omega}) \, \delta(\hat{\Omega} - \hat{N}) \, Y_{Q,0,m}(\hat{\Omega}) = Y^*_{Q,0,m'}(\hat{N}) \, Y_{Q,0,m}(\hat{N}) = \\
&= \frac{2l+1}{4\pi} \begin{pmatrix} 2l \\ l+m' \end{pmatrix}^{\frac{1}{2}} \begin{pmatrix} 2l \\ l+m \end{pmatrix}^{\frac{1}{2}} \left(\frac{1-x}{2}\right)^{\frac{l-m}{2}} \left(\frac{1+x}{2}\right)^{\frac{l+m}{2}} \cdot \\
&\quad \left(\frac{1-x}{2}\right)^{\frac{l-m'}{2}} \left(\frac{1+x}{2}\right)^{\frac{l+m'}{2}} P_0^{l-m,l+m}(x) \, P_0^{l-m',l+m'}(x) \, e^{i(m-l)\phi} \, e^{i(m'-l)\phi} = \\
&= \delta_{l,m}\delta_{l,m'} \frac{2l+1}{4\pi} P_0^{0,2l}(x) \, P_0^{0,2l}(x) = \frac{2l+1}{4\pi} \delta_{l,m}\delta_{l,m'}. \qquad (6.8)
\end{aligned}$$

From Eqs. 6.7-6.8, ignoring the overall coupling constant AA' (which is independent of the system size, R or Q), the transverse part of F projected onto the lowest LL simplifies to

$$F = c^\dagger_{l\downarrow} c_{l\uparrow} + c^\dagger_{l\uparrow} c_{l\downarrow}. \qquad (6.9)$$

Clearly, the change of the localized (nuclear) spin is accompanied by a reversal of an electronic spin spread over a (cyclotron) orbit of finite radius $\sim \lambda$.

The oscillator strength τ^{-1} of the transition between the initial and final electronic eigenstates is (by the Fermi golden rule) proportional to the square of the matrix element of F. We define,

$$\tau_{if}^{-1} = |{}_e\langle f| \, F \, |i\rangle_e|^2 , \qquad (6.10)$$

and accordingly the spectral function $\tau^{-1}(E) \equiv \tau_i^{-1}(E) = \sum_f \tau_{if}^{-1} \delta(E - (E_i - E_f))$, where E_i and E_f are the energies of the initial and final electronic state, respectively. Due to the simple form of the operator F in our basis (6.9), the matrix element (6.10) can be easily evaluated for any known pair of $|i\rangle_e$ and $|f\rangle_e$ eigenstates. Therefore, the most difficult computational task is the accurate calculation of the many-electron eigenfunctions. Moreover, because of the breaking of both spatial and spin symmetry by the transition operator F, entire multiplets with different L_z and S_z must be calculated

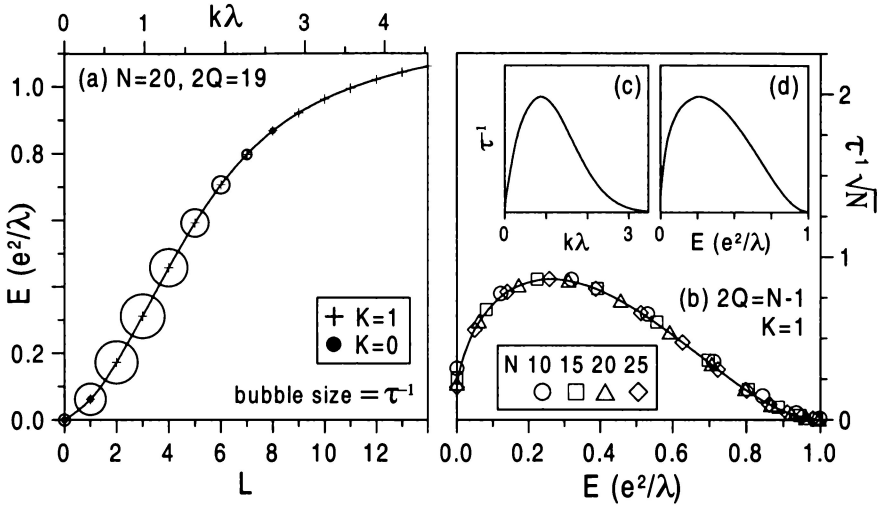


Figure 6.1: Transitions from the $\nu = 1$ Laughlin ground state induced by hyperfine interaction with a localized spin. (a) The energy E of transitions vs angular momentum L and wave vector $k\lambda$ for a system of $N = 20$ electrons filling exactly the lowest LL ($2Q = 19$). Bubble size is proportional to τ^{-1}. Solid dots and crosses mark states with $K = 0$ and 1 reversed spins, respectively. (b) The transition probability (normalized by $\sqrt{N}$) as a function of energy E for $N \leq 25$. (c) and (d) The spectral functions $\tau^{-1}(k\lambda)$ and $\tau^{-1}(E)$, respectively, in the planar geometry limit ($N \to \infty$). [107]

for each L and S. Hence, the proper identification of the relevant many-electron eigenstates that: (i) describe a planar system in the $R/\lambda \to \infty$ limit, (ii) have significant τ^{-1}, becomes essential.

6.3 Integral Quantum Hall Regime

We begin with the integral quantum Hall regime and the filling factor of precisely $\nu = 1$. We evaluate numerically the matrix elements (6.10) for all possible transitions induced by the operator F from the initial ferromagnetic ground state (GS) of the system. The results for $N = 20$ electrons at $2Q = N - 1 = 19$ are shown in Fig. 6.1(a). In this and all the other spectra in this chapter E stands for the energy difference between the final

and initial states and is given in the units of $E_C = e^2/\lambda$. The Zeeman energy is not included. The bubble size corresponds to τ_{if}^{-1}, where i is the GS. We show that the only final states with possibly nonzero transition probability are the SW's with the number of reversed spins $K = 1$.

To determine the spectral function of an infinite 2DEG we have compared data obtained for different electron numbers, $N \leq 25$, and plotted the results in Fig. 6.1(b). τ_{if}^{-1} for discrete values of E is multiplied by the factor $\sqrt{N} \propto \sqrt{Q} \propto R/\lambda$, which comes from normalization of the wave function of the extended SW over the entire sphere. All data points lie on one regular curve, which allows prediction of their behavior in the planar system, $N \to \infty$ (see insets (c) and (d)).

The following observations can be made for a 2DEG at precisely $\nu = 1$: (i) The hyperfine interaction F with a localized spin creates a SW whose energy spectrum begins at the electron Zeeman gap ($E \geq E(k = 0) = E_Z$). (ii) The function $\tau^{-1}(k)$ vanishes at $k = 0$ and $k \to \infty$, and has a maximum at a finite value of k. We found it to be at $k_0 \sim 1/\lambda$, which is consistent with the fact that the change of the total electron spin is spread over a region of radius $\sim \lambda$ (a cyclotron orbit). (iii) The maximum of $\tau^{-1}(E)$ is at the energy larger than $E(0) = E_Z$ by a term of the order of $E_C = e^2/\lambda$. Since the nuclear Zeeman energy is much smaller than both E_C and E_Z, energy conservation law prevents flipping nuclear spins at (locally) $\nu = 1$, even at arbitrarily small E_Z. This explains long relaxation times observed in experiments at this filling factor [5, 74, 110].

As discussed in Sec. 5, adding an extra particle (a reversed-spin electron or a hole) to the $\nu = 1$ ferromagnetic GS will cause the formation of skyrmions. Importantly, the skyrmionic spin excitation gap will be significantly reduced compared to E_Z and therefore, unlike SW's of the $\nu = 1$ fluid, skyrmions are expected to play an important role in the relaxation processes of nuclear spins. Skyrmions are well-defined charged quasiparticles which move freely in the underlying $\nu = 1$ fluid, and because of the Laughlin correlations between them, at low density they remain virtually unperturbed by the skyrmion-skyrmion scattering [33, 125]. The collisions of a nucleus with more

than one skyrmion can be therefore excluded from coupling of a 2DEG to nuclear spins [125].

To determine the contribution from collisions with skyrmions to nuclear relaxation processes, we calculated matrix elements (6.10) for transitions from a GS of 2DEG at $\nu = 1^{\pm}$ to all possible final states. We investigated systems with different N and found that the dominant contribution comes from the internal excitations of skyrmions in which their number of reversed spins change by one, $S_K \to S_{K\pm1}$.

We continue with the example of $N = 12$ electrons and one hole in the lowest LL ($l = 6$) at $2Q = 12$. In Fig. 6.2 we show transition probabilities from the states containing one skyrmion with $K = 0$ ($S_0^+ = h$) (a), $K = 1$ (S_1^+) (b,c), $K = 2$ (S_2^+) (d) to all possible final states. The GS of the ferromagnetic system (a) is characterized by $L = S = 6$ and on the Haldane sphere $L_z = -5$ corresponds to the h positioned on the orbital next to the north pole (e.g. to the localized spin). The highest intensity in the spectrum has the transition to the S_1^+ state. Since the Coulomb energy E of this transition is negative, setting the appropriate electronic Zeeman gap can make the total energy $E + E_Z$ equal to nuclear Zeeman splitting.

In Fig. 6.2(b) we consider transitions from the state containing one S_1^+. The peak with a negative Coulomb energy and simultaneously the highest weight can be identified among final states of 2DEG (see inset) as S_2^+ ($L = S = 4$). The other transitions present in the spectrum occur at Coulomb energies greater than zero and large compared to the nuclear Zeeman gap, which, as in the case of precisely $\nu = 1$, excludes them from the spin flip scattering with the nucleus. The value of $L_z = -4$ corresponds to the S_1^+ is placed at the orbital next to the north pole. Not surprisingly, moving S_1^+ away from the north pole (localized spin) to $L_z = -2$ weakens the S_1^+-S_2^+ transition, which is shown in Fig. 6.2(c). The energy spectrum and intensities of transitions to corresponding final states from the initial S_2^+ GS are shown in Fig. 6.2(d). It is clear that most of the transition probability goes to a well-defined final state S_3^+ ($L = S = 3$), with a negative excitation energy, .

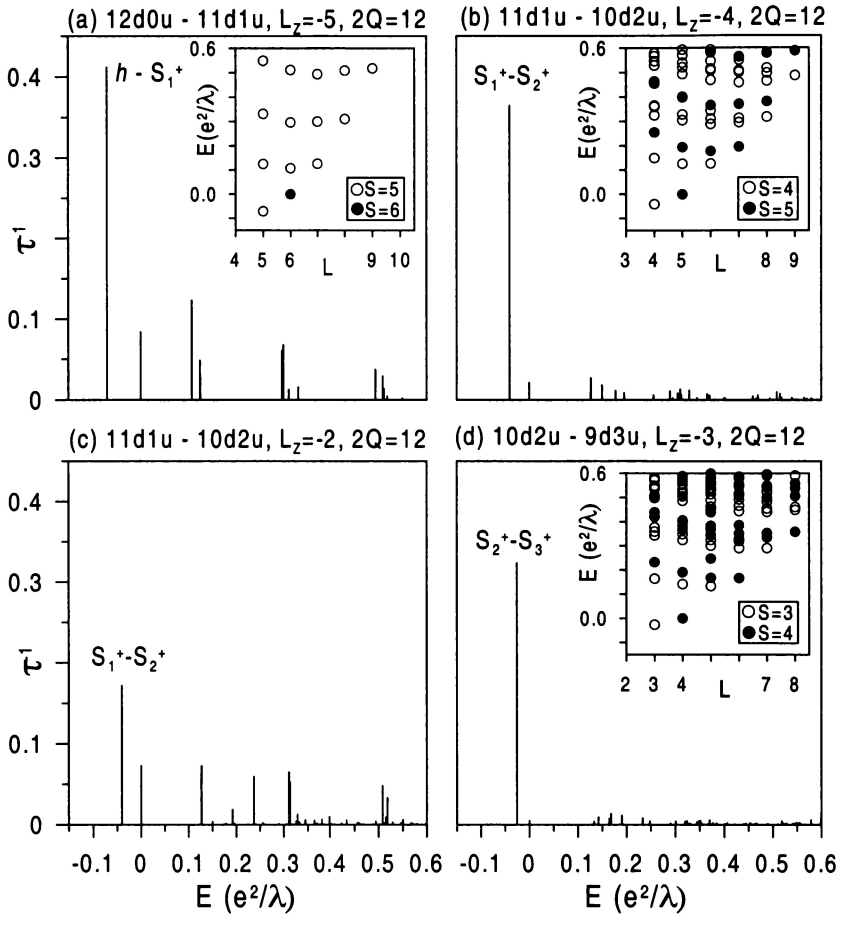


Figure 6.2: The intensity τ^{-1} vs energy E and the energy spectra (insets) of $N = 12$ electrons at $2Q = 12$ ($\nu = 1^{\pm}$) for transitions from initial states: (a) $K = 0, L_z = -5$ (a h next to the nucleus), (b)$K = 1, L_z = -4$ (S_1^+ next to the nucleus) (c)$K = 1, L_z = -2$ (S_1^+ moved away from the nucleus) (d)$K = 1, L_z = -3$ (S_2^+ at the nucleus). The d and u symbols correspond to the $\downarrow$- and $\uparrow$-spin polarization. [107]

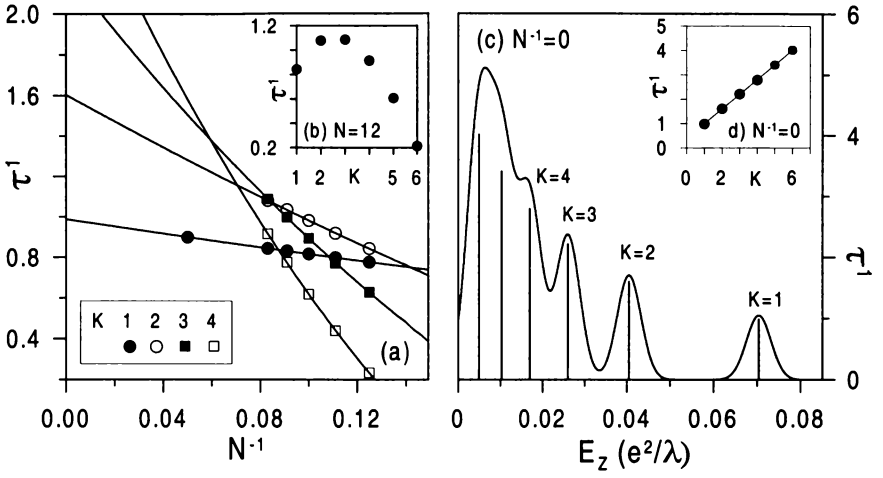


Figure 6.3: Intensities of transitions in the $\nu = 1^{\pm}$ fluid in the limit of $N^{-1} \to 0$. (a) The intensity τ^{-1} vs N^{-1} for transitions from the skyrmion states with $K \leq 4$ (marked with different symbols) to final states with $K \pm 1$ due to the hyperfine interaction with a nucleus. (b) The transition probability τ^{-1} between skyrmionic states $K \to K \pm 1$ vs K in a system of $N = 12$ electrons. (c) The intensity of transitions $K \to K \pm 1$ as a function of the Zeeman energy. K is the number of reversed spins in the initial state; the solid line is a Gaussian expected to be observed in experiment. (d) Same as (b) but in the $N^{-1} \to 0$ limit (planar system). [107]

We found that the spin scattering probability τ^{-1} of a S_K (of size $\propto \lambda$) by a localized spin, depends on the impact parameter which is proportional to L_z (see the example in Fig. 6.2(c-d)). Because a skyrmion can move freely in the underlying $\nu = 1$ 2DEG and the external localized spin was placed at the north pole by an arbitrary choice, it is more physical to consider probabilities τ^{-1} summed over all possible impact parameters L_z.

We showed that in finite size systems at $\nu = 1^{\pm}$ the electron spin excitations coupled to the excitations of nuclear spins are the internal skyrmion transitions $S_K \to S_{K+1}$. The dependence of these intensities (summed over all possible L_z) on the number of reversed spins K in the final state for a system of $N = 12$ electrons is shown in Fig. 6.3(b). Quite surprisingly, the function $\tau^{-1}(K)$ has a maximum at a finite K. In order to esti-

mate τ^{-1} in an infinite system, we calculated matrix elements (6.10) of the $S_K \to S_{K+1}$ transition for different N. The results are shown in Fig. 6.3(a) (different symbols mark different K's). It is remarkable that τ^{-1} shows a very regular dependence on N^{-1}. Extrapolation to $N^{-1} \to 0$ limit shows that on the infinite plane the $S_K \to S_{K+1}$ transitions will prevail. The extrapolated intensities are shown in Fig. 6.3(d). Noticeably, τ^{-1} is an almost linear and increasing function of K. This is the consequence of the fact that the $S_K \to S_{K+1}$ transition is an edge excitation and thus τ^{-1} summed over all impact parameters L_z, should increase with the circumference of the skyrmion and therefore with K. That τ^{-1} has a maximum at a finite K in finite systems is an artifact of the chosen geometry, as the circumference of a skyrmion decreases with increasing K when it occupies more than half of the sphere.

Because in experiment the differential cross-section for skyrmion-nucleus collisions also depends on the skyrmion circumference, one can expect that τ^{-1} will increase as a function of K. In Fig. 6.3(c) we show intensity peaks for subsequent K's as a function of E_Z and we add a sample Gaussian to imitate the experimental broadening. It is remarkable that when the value of E_Z is lowered peaks with higher K are selected from the spectral function, the separation between them decreases whereas their intensities increase. Let us stress that these results are qualitatively different from the case of precisely $\nu = 1$.

6.4 Fractional Quantum Hall Regime

It has been shown experimentally [24, 57, 53] that at filling factors close to $\nu = \frac{1}{3}$ there are electron polarization changes resembling those due to skyrmions at $\nu = 1$. It is therefore expected that the fast and weakly temperature-dependent nuclear spin relaxation [6, 23] observed at filling factors $\nu = \frac{1}{3}^{\pm}$ is due to the coupling to skyrmions and anti-skyrmions.

We investigated a number of finite size systems and we found that flipping a localized spin in the $\nu = \frac{1}{3}$ state creates a SW, in perfect analogy to the case of $\nu = 1$. As an

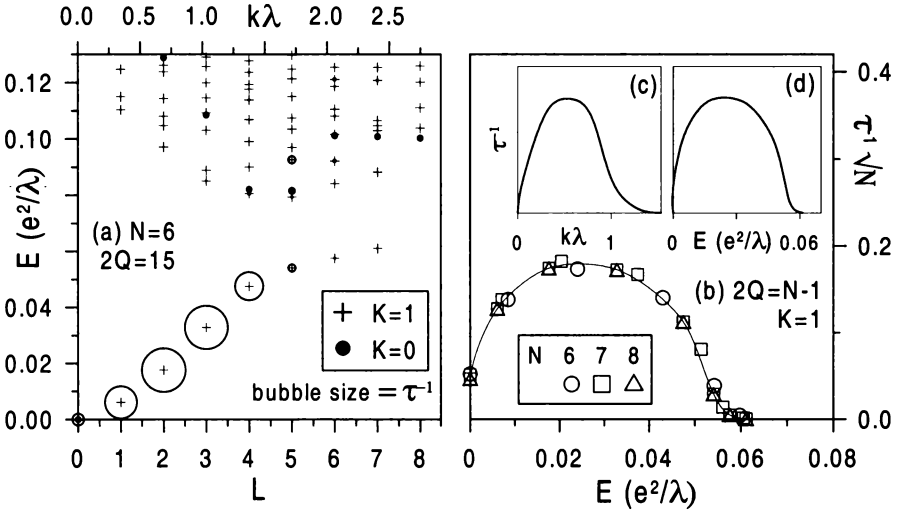


Figure 6.4: Transitions from the $\nu = \frac{1}{3}$ ground state. (a) The energy E of transition from the ferromagnetic GS of the system of $N = 6$ electrons at $2Q = 15$ ($\nu = \frac{1}{3}$) as a function of angular momentum L and wave vector $k\lambda$. The final states have $K = 0$ (solid dots) and $K = 1$ (open circles) number of reversed spins, respectively. Bubble size corresponds to the transition intensity τ^{-1}. (b) The transition probability (normalized by $\sqrt{N}$) vs energy E for $N \leq 8$. The spectral functions $\tau^{-1}(k\lambda)$ and $\tau^{-1}(E)$ in the planar system (infinite Haldane sphere) are shown in (c) and (d). [107]

example, a system of $N = 6$ electrons at $2Q = 15$ is shown if Fig. 6.4(a). The effective monopole strength is $2Q^* = 2Q - 2(N-1) = 5$ and six CF's fill exactly their lowest spin-$\downarrow$ LL of degeneracy $g^* = 2Q^* + 1 = 6$. The bubble size in the plot is proportional to τ_{if}^{-1} (6.10) for transitions from the ferromagnetic GS ($K = 0$) to all possible final states ($K = 1$).

As shown in Fig. 6.4(b) the function τ^{-1} (again normalized by $\sqrt{N}$, compare $\nu = 1$ in Fig. 6.1) has a very regular dependence on N. Hence, we were able to predict its shape in an infinite planar system (see insets (c) and (d)). The spectral function vanishes for $k \to 0$ or ∞ and has a maximum at a finite k. This maximum is at $k \sim \left(\sqrt{3}\lambda\right)^{-1}$, which is because the change of the total electron spin at $\nu = \frac{1}{3}$ is spread over the area of 3 cyclotron orbits.

By similar argument as in the case of $\nu = 1$, energy conservation will prevent coupling of nuclear spins to spin excitations at (locally) $\nu = \frac{1}{3}$, which explains long relaxation times observed in experiments.

Our study of finite systems at filling factors $\nu = \frac{1}{3}^{\pm}$ indicates that the dominant contribution to collisions with a localized spin comes from internal transitions of skyrmions, $S_K \to S_{K\pm1}$. The filling factor $\nu = \frac{1}{3}^{\pm}$ corresponds to one QH or $\mathrm{QE_R}$ in the $n = 0$ CF LL or a QE in the first excited $n = 1$ CF LL. These cases need be considered separately because of the absence of the particle–hole symmetry in the CF LL.

We illustrate our results on the example of $N = 6$ electrons (Fig. 6.5). We begin the discussion with the ferromagnetic CF GS with an extra QH present in the lowest CF LL of degeneracy $g^* = 2Q^* + 1 = 2Q - 2(N-1) + 1 = 7 = N + 1$ (Fig. 6.5(a)). Here, $L_z = -2$ corresponds to one QH placed at the next orbital to the north pole. The transition with a negative Coulomb energy can be identified in the inset as leading to the final state with $L = S = 2$, which is the anti-skyrmion S_1^+. In Fig. 6.5(b) we show the energy spectrum and the intensities of transitions from the GS of a system where one QE was added to a $\nu = \frac{1}{3}$ Laughlin fluid. The only peak with a negative Coulomb energy is also the one with the highest intensity and describes the QE–$\mathrm{QE_R}$ transition.

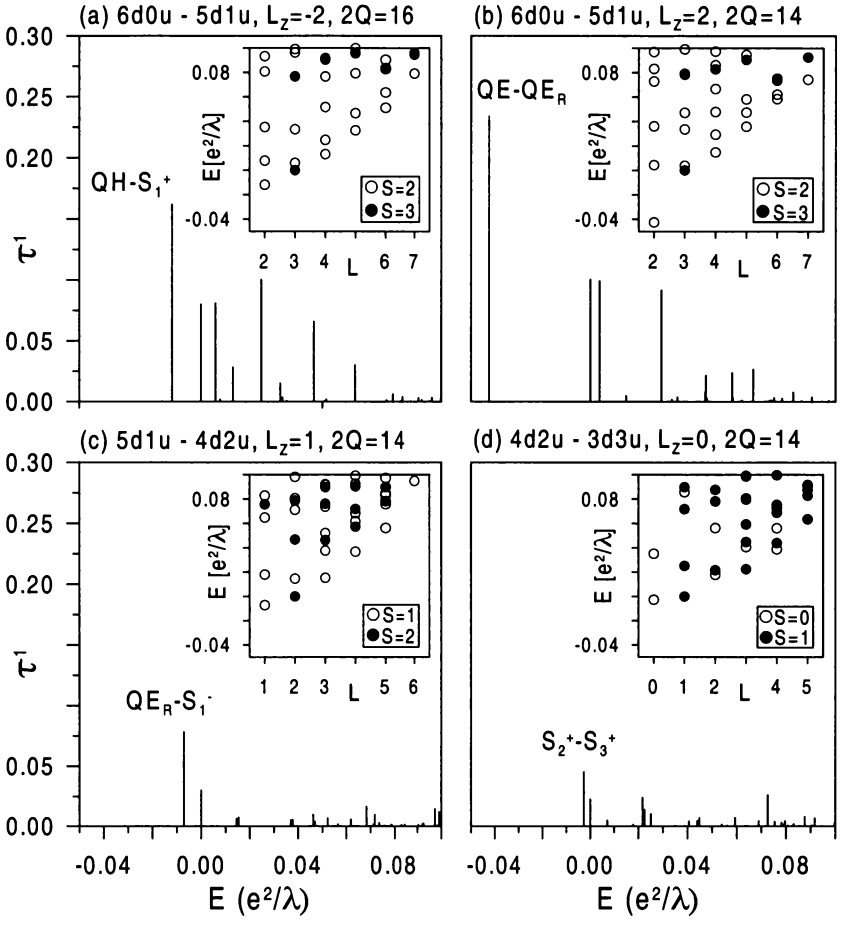


Figure 6.5: τ^{-1} vs energy E and the energy spectra (insets) of the system of $N = 6$ electrons at $\nu = \frac{1}{3}^{\pm}$ for the transitions from the following initial states: (a) QH in the $n = 0$ spin-$\downarrow$ LL ($2Q = 16$), (b) QE in the first excited spin-$\downarrow$ LL ($2Q = 14$), (c) QE_R in the $n = 0$ spin-$\uparrow$ LL ($2Q = 14$), (d) skyrmion S_2^+ (two SW's bound to a QH, $2Q = 14$). The d and u symbols correspond to the $\downarrow$- and $\uparrow$-spin polarization. [107]

The spectrum for a process in which a localized spin is changed simultaneously with creating in the 2DEG an additional QH–QE_R pair (SW) in the presence of a QE_R to form a skyrmion S_1^-, is presented in Fig. 6.5(c). In Fig. 6.5(d) it is shown that the S_2^+ skyrmion can bind another SW and form S_3^+. Again, as at $\nu = 1$, because the spin scattering probability of a skyrmion by a localized spin depends on the impact parameter, it is τ^{-1} summed over all possible L_z that will have a physical meaning. All excitations of the type QH$\rightarrow S_1^+ \rightarrow S_2^+ \ldots$ or QE$\rightarrow$QE$_R \rightarrow S_1^- \ldots$ have negative Coulomb energies. Therefore, even in the presence of finite E_Z, the total energy can be made equal to the nuclear Zeeman gap, which is essentially different from the case of a locally incompressible $\nu = \frac{1}{3}$ filling factor. The mechanism discussed here is responsible for fast nuclear spin relaxation at $\nu = \frac{1}{3}^{\pm}$.

Bibliography

Bibliography

[1] Y. Aharonov, D. Bohm, Phys. Rev. B **115**, 485 (1959).

[2] E. H. Aifer, B. B. Goldberg, D. A. Broido, Phys. Rev. Lett. **76**, 680 (1996).

[3] V. M. Apalkov, T. Chakraborty, P. Pietiläinen, and K. Niemelä, unpublished (preprint cond-mat/0007168v2).

[4] J. E. Avron, I. W. Herbst, B. Simon, Ann. PHys. **114**, 431 (1978).

[5] S. E. Barrett, G. Dabbagh, L. N. Pfeiffer, K. W. West, and R. Tycko, Phys. Rev. Lett. **74**, 5112 (1995).

[6] V. Bayot, E. Grivei, S. Melinte, M. B. Santos, M. Shayegan, Phys. Rev. Lett. **76**, 4584 (1996).

[7] P. Beran and R. Morf, Phys. Rev. B **43**, 12654 (1991).

[8] *Introduction to Quantum Computers*, G. P. Berman, G. D. Doolen, R. Mainieri, V. I. Tsifrinovich (World Scientific, Singapore, 1998).

[9] G. P. Berman, F. Borgonovi, F. M. Izrailev, V. I. Tsifrinovich, preprint quant-ph/0012106

[10] A. Berg, M. Dobers, R. R. Gerhards and K. V. Klitzing, Phys. Rev. Lett. **64**, 2563 (1990).

[11] L. Brey, H. A. Fertig, R. Côté, A. H. MacDonald, Phys. Rev. Lett. **75**, 2562 (1995).

[12] R. L. Brockbank, H. D. M. Davies, J. F. Ryan, M. A. Thomson, A. J. Turberfield, Physica E **6**, 56 (2000).

[13] Yu. A. Bychkov, S. V. Iordanskii, and G. M. Eliashberg, Pis'ma Zh. Eksp. Teor. Fiz. **33**, 152 (1981) [Sov. Phys.—JETP Lett. **33**, 143 (1981)].

[14] T. Chakraborty, F. C Zhang, Phys. Rev. B **29**, 7032 (1984).

[15] T. Chakraborty, P. Pietiläinen, and F. C. Zhang, Phys. Rev. Lett. **57**, 130 (1986).

[16] T. Chakraborty and P. Pietiläinen, Phys. Rev. B **41**, 10862 (1990).

[17] T. Chakraborty and P. Pietiläinen, *The Quantum Hall Effects*, (Springer-Verlag, New York, 1995).

[18] A. M. Chang, P. Berglund, D. C. Tsui, H. L. Störmer, J. C. Hwang, Phys. Rev. Lett. **53**, 997 (1984).

[19] X. M. Chen and J. J. Quinn, Phys. Rev. Lett. **70**, 2130 (1993); Phys. Rev. B **50**, 2354 (1994); Phys. Rev. B **51**, 5578 (1995).

[20] X. M. Chen, J. J. Quinn, Solid St. Commun. **92**, 865 (1996).

[21] R. G. Clark, R. J. Nicholas, A. Usher, C. T. Foxon, J. J. Harris, Surface Science **170**, 141 (1986).

[22] R. G. Clark, S. R. Haynes, A. M Suckling, J. R. Mallett, P. A. Wright, J. J. Harris, and C. T. Foxon, Phys. Rev. Lett. **62**, 1536 (1989).

[23] R. Côté, A. H. MacDonald, L. Brey. H. A. Fertig, S. M. Girvin, H. T. C. Stoof, Phys. Rev. Lett. **78**, 4825 (1997).

[24] H. D. M. Davies, R. L. Brockbank, J. F. Ryan, A. J. Turberfield, Physica B **256-258**, 104 (1998).

[25] P. A. M. Dirac, Proc. R. Soc. London, Ser. A **133**, 60 (1931).

[26] D. P. DiVincenzo, Science **270**, 255 (1995);

[27] A. B. Dzyubenko, Solid State Commun. **113**, 683 (2000).

[28] G. Ebert, K. von Klitzing, J. C. Maan, G. Remenyi, C. Probst, G.Weimann, W. Schlapp, J. Phys. C, **17**, L775 (1984).

[29] J. P. Eisenstein, H. L. Störmer, L. N. Pfeiffer, and K. W. West, Phys. Rev. Lett. **62**, 1540 (1989); Phys. Rev. B **41**, 7910 (1990).

[30] L. W. Engel, S. W. Hwang, T. Sajoto, D. C. Tsui, and M. Shayegan, Phys. Rev. B **45**, 3418 (1992).

[31] G. Fano, F. Ortolani, E. Colombo, Phys. REv. B **34**, 2670 (1986).

[32] H. A. Fertig, L. Brey, R. Côté, A. H. MacDonald, Phys. Rev. B **50**, 11018 (1994).

[33] H. A. Fertig, L. Brey, R. Côté, and A. H. MacDonald, Phys. Rev. Lett. **77**, 1572 (1996).

[34] A. Garg, Phys. Rev. Lett. **77**, 964 (1996).

[35] L. P. Gor'kov and I. E. Dzyaloshinskii, Zh. Eksp. Teor. Fiz. **53**, 717 (1967) [Sov. Phys.—JETP **26**, 449 (1968)].

[36] F. D. Haldane, Phys. Rev. B **51**, 605 (1983).

[37] F. D. M. Haldane, Phys. Rev. Lett. **51**, 605 (1983).

[38] F. D. M. Haldane, E. H. Rezayi, Phys. Rev. Lett. **54**, 237 (1985); Phys Rev. B **31**, 2529 (1985); Phys. Rev. Lett. **60**, 956 (1988).

[39] F. D. M. Haldane, in Ref. [86], chap. 8, p. 303.

[40] B. I. Halperin, Helv. Phys. Acta **56**, 75 (1983).

[41] B. Halperin, Phys. Rev. Lett. **52**, 1583 (1984); **52**, 2390 (E).

[42] B. I. Halperin, P. A. Lee, N. Read, Phys. Rev. B **47**, 7312 (1993).

[43] R. M. Hannak, M. Oestreich, A. P. Heberle, W. W. Ruhle, K. Kohler, Solid State Commun. **93**, 3132 (1995).

[44] R. Haydock, Solid St. Phys. **35**, 215 (1980).

[45] A. Imamoglu, D. D. Awschalom, G. Burkard, D. P. DiVincenzo, D. Loss, M. Sherwin, A. Small, Phys. Rev. Lett. **83**, 4204 (1999); R. Vrijen, E. Yablonovitch, K. Wang, H. W. Jiang, A. Balandin, V. Roychowdhury, T. Mor, D. P. DiVincenzo, Phys. Rev. A **62**, 012306 (2000).

[46] J. K. Jain, R. K. Kamilla, *Composite Fermions in the Hilbert Space of the Lowest Electronic Landau Level*, preprint cond-mat/9704031.

[47] J. K. Jain, Phys. Rev. Lett. **63**, 199 (1989); Phys. Rev. B **40**, 8079 (1990); Science **266**, 1199 (1994).

[48] J. K. Jain, V. J. Goldman, Phys. Rev. B **45**, 1255 (1992).

[49] C. Kallin and B. I. Halperin, Phys. Rev. B **30**, 5655 (1984).

[50] V. Kalmeyer, S. Zhang, Phys. Rev. B **46**, 9889 (1992).

[51] R. K. Kamilla, X. G. Wu, J. K. Jain, Solid State Commun. **99**, 289 (1996)

[52] B. E. Kane, Nature **393**, 133 (1998).

[53] P. Khandelwal, N. N. Kuzma, S. E. Barrett, L. N. Pfeiffer, and K. W. West, Phys. Rev. Lett. **81**, 673 (1998).

[54] P. Khandelwal, A. E. Dementyev, N. N. Kuzma, S. E. Barrett, L. N. Pfeiffer, K. W. West, Phys. Rev. Lett. **86**, 5353 (2001).

[55] K. von Klitzing, G. Dorda, M. Pepper, Phys. Rev. Lett. **45**, 494 (1980).

[56] I. V. Kukushkin, R. J. Haug, K. von Klitzing, K. Ploog, Phys. Rev. Lett. **72**, 736 (1994).

[57] N. N. Kuzma, P. Khandelwal, S. E. Barrett, L. N. Pfeiffer, K. W. West, Science **281**, 686 (1998);

[58] C. Lanczos, J. Res. natn. Bur. Stand. **45**, 255 (1950).

[59] L. D. Landau Zeitschrift für Physik **64**, 629 (1930).

[60] L. D. Laundau, E. M. Lifszyc *Mechanika Kwantowa*, PWN Warszawa (1979).

[61] R. B. Laughlin, Phys. Rev. B **23**, 5632 (1981).

[62] R. B. Laughlin, Phys. Rev. Lett. **50**, 1395 (1983).

[63] R. B. Laughlin, Phys. Rev. B. **27**, 3383 (1983).

[64] R. B. Laughlin, Surface Science **141**, 11 (1984).

[65] D. R. Leadley, R. J. Nicholas, D. K. Maude, A. N. Utjuzh, J. C. Portal, J. J. Harris, and C. T. Foxon, Phys. Rev. Lett. **79**, 4246 (1997).

[66] D. H. Lee and C. L. Kane, Phys. Rev. Lett. **64**, 1313 (1990).

[67] A. Lopez, E. Fradkin, Phys. Rev. B **44**, 5246 (1991); Phys. Rev. Lett. **69**, 2126 (1992); Phys. Rev. B. **47**, 7080 (1993).

[68] D. Loss and D. P. DiVincenzo, Phys. Rev. A **57**, 120 (1998).

[69] A. H. MacDonald, H. A. Fertig, L. Brey, Phys. Rev. Lett. **76**, 2153 (1996).

[70] A. H. MacDonald and J. J. Palacios, Phys. Rev. B **58**, R10171 (1998).

[71] A. H. MacDonald, E. H. Rezayi, Phys. Rev. B **42**, 3224 (1990).

[72] J. R. Mallet, R. G. Clark, R. J. Nicholas, R. L. Willet, J. J. Harris, C. T. Foxon, Phys. Rev. B **38**, 2200 (1988).

[73] M. J. Manfra, E. H. Aifer, B. B. Goldberg, D. A. Broido, L. Pfeiffer, K. West, Phys. Rev. B **54**, R17327 (1996).

[74] T. Maniv, Y. A. Bychkov, I. D. Vagner, P. Wyder, preprint cond-mat/0011361.

[75] D. K. Maude, M. Potemski, J. C. Portal, M. Henini, L. Eaves, G. Hill, M. A. Pate, Phys. Rev. Lett. **77**, 4604 (1996).

[76] E. E. Mendez, M. Heiblum, L. L. Chang, L. Esaki, Phys. Rev. B **28**, 4886 (1983).

[77] E. E. Mendez, L. L. Chang, M. Heiblum, L. Esaki, M. Nahughton, M. Martin, J. Brooks, Phys. Rev. B **30**, 7310 (1984).

[78] K. Moon, H. Mori, K. Yang, S. M. Girvin, A. H. MacDonald, L. Zheng, D. Yoshioka, S. C. Zhang, Phys. Rev. B **51**, 5138 (1995).

[79] D. Mozyrsky, V. Privman, M. L. Glasser Phys. Rev. Lett. **86**, 5112 (2001).

[80] D. Mozyrsky, V. Privman, I. D. Vagner, Phys. Rev. B **63**, 085313 (2001).

[81] J. H. Oaknin, L. Martin-Moreno, C. Tejedor, Phys. Rev. B **54**, 16850 (1996).

[82] J. J. Palacios, L. Martin-Moreno, G. Chiappe, E. Louis, C. Tejedor, Phys. Rev. B **50**, 5760 (1994).

[83] J. J. Palacios, D. Yoshioka, A. H. MacDonald, Phys. Rev. B **54**, 2296 (1996).

[84] G. M. Palma, K. A. Suominen, A. K. Ekert, Proc. Royal Soc. London A **452**, 567 (1996).

[85] K. Park and J. K. Jain, Phys. Rev. B **62**, 13274 (2000).

[86] R. E. Prange, S. M. Girvin, *The Quantum Hall Effect*, Springer-Verlag, New York (1987).

[87] V. Privman, D. Mozyrsky, I. D. Vagner, preprint cond-mat/0102308.

[88] V. Privman, I. D. Vagner and G. Kventsel, Phys. Lett. A **239**, 141 (1998)

[89] J. J. Quinn and A. Wójs, J. Phys.: Cond. Mat. **12**, R265 (2000).

[90] R. Ramajaran, *Solitons and Instantons* (North-Holland, Amsterdam, 1982)

[91] E. H. Rezayi, Phys. Rev. B **36**, 5454 (1987); Phys. Rev. B **43**, 5944 (1991).

[92] T. Sajoto, Y. W. Suen, L. W. Engel, M. B. Santos, M. Shayegan, Phys. Rev. B **41**, 8449 (1990).

[93] J. J. Sakurai *Modern Quantum Mechanics*, The Benjamin/Cumming Publishing Company, Inc. (1985).

[94] M. Shayegan, J. Jo, Y. W. Suen, M. Santos, V. J. Goldman, Phys. Rev. Lett. **65**, 2916 (1990).

[95] S. P. Shukla, M. Shayegan, S. R. Parihar, S. A. Lyon, N. R. Cooper, A. A. Kiselev, Phys. Rev. B **61**, 4469 (2000).

[96] J. Sinova, S. M. Girvin, T. Jungwirth, K. Moon, Phys. Rev. B **61**, 2749 (2000).

[97] P. Sitko, S. N. Yi, K. S. Yi, J. J. Quinn, Phys. Rev. Lett. **76**, 3396 (1996).

[98] P. Sitko, K.-S. Yi, and J. J. Quinn, Phys. Rev. B **56**, 12417 (1997).

[99] T. Skyrme, Proc. R. Soc. London A **262**, 237 (1961).

[100] *Principles of Magnetic Resonance*, C. P. Slichter (Springer-Verlag, New York, 1990).

[101] M. J. Snelling, G. P. Flinn, A. S. Plaut, R. T. Harley, A. C. Tropper, R. Eccleston, and C. C. Phillips, Phys. Rev. B **44**, 11345 (1991).

[102] S. L. Sondhi, A. Karlhede, S. A. Kivelson, and E. H. Rezayi, Phys. Rev. B **47**, 16419 (1993).

[103] H. L. Störmer, A. M. Chang, D. C. Tsui, J. C. Hwang, A. C. Gossard, W. Wiegmann, Phys. Rev. Lett. **50**, 1953 (1983).

[104] H. L. Störmer, Bull. Am. Phys. Soc. **45**, 643 (2000).

[105] I. Szlufarska, A. Wójs, J. J. Quinn, Phys. Rev. B **64**, 165318 (2001).

[106] I. Szlufarska, A. Wójs, J. J. Quinn, *Reversed-spin quasiparticles in fractional quantum Hall systems and their effect on photoluminescence*, to appear in Physica E.

[107] I. Szlufarska, A. Wójs, J. J. Quinn, *Hyperfine coupling of intergral and fractional quantum Hall states to nuclear spins: A finite size study*, preprint: cond-mat/0203160.

[108] D. C. Tsui, H. L. Störmer, A. C. Gossard, Phys. Rev. Lett. **48**, 1559 (1982).

[109] I. S. Tupitsyn, N. V. Prokofev, P. C. E. Stamp, Int. J. Modern Phys. B **11**, 2901 (1997).

[110] R. Tycko, S. E. Barrett, G. Dabbagh, L. N. Pfeiffer, K. W. West, Science **268**, 1460 (1995).

[111] I. D. Vagner and T. Maniv, Phys. Rev. Lett. **61**, 1400 (1988).

[112] R. Willett, J. P. Eisenstein, H. L. Störmer, D. C. Tsui, A. C. Gossard, and J. H. English, Phys. Rev. Lett. **59**, 1776 (1987).

[113] A. Wójs, P. Hawrylak, Phys. Rev. B **51**, 10880 (1995).

[114] A. Wójs, P. Hawrylak, Phys. Rev. B **56**, 13227 (1997).

[115] A. Wójs, J. J. Quinn, Solid State Commun. **108**, 493 (1998).

[116] A. Wójs, J. J. Quinn, Physica E **3**, 181 (1998).

[117] A. Wójs, P. Hawrylak, J. J. Quinn, Phys. Rev. B **60**, 11661 (1999).

[118] A. Wójs, I. Szlufarska, K.-S. Yi, J. J. Quinn, Phys. Rev. B **60**, 11273 (1999).

[119] A. Wójs, J. J. Quinn, Phil. Mag. B **80**, 1405 (2000).

[120] A. Wójs, J. J. Quinn, Phys. Rev. B **61**, 2846 (2000).

[121] A. Wójs, J. J. Quinn, and P. Hawrylak, Phys. Rev. B **62**, 4630 (2000).

[122] A. Wójs, Phys. Rev. B **63**, 235322 (2001).

[123] A. Wójs and J. J. Quinn, Phys. Rev. B **63**, 045303 (2001); Phys. Rev. B **63**, 045304 (2001); Solid State Commun. **118**, 225 (2001).

[124] A. Wójs, Phys. Rev. B **63**, 125312 (2001).

[125] A. Wójs, J. J. Quinn, preprint: cond-mat/0109549

[126] T. T. Wu, C. N. Yang, Nucl. Phys. B **107**, 365 (1976).

[127] X. G. Wu, G. Dev, and J. K. Jain, Phys. Rev. Lett. **71**, 153 (1993).

[128] X. C. Xie, Yin Guo, F. C. Zhang, Phys. Rev. B **40**, 3487 (1989).

[129] X. C. Xie, S. He, Phys. Rev. B **53**, 10019 (1996).

[130] A. S. Yeh, H. L. Störmer, D. C. Tsui, L. N. Pfeiffer, K. W. Baldwin, K. West, Phys. Rev. Lett. **82**, 592 (1999).

[131] K. S. Yi, P. Sitko, A. Khurana, J. J. Quinn, Phys. Rev. B **54**, 16432 (1996).

[132] D. Yoshioka, Prog. Theor. Phys. **81**, 97 (1985).

[133] D. Yoshioka, Physica E **6**, 83 (2000).

[134] F. C. Zhang, T. Chakraborty, Phys. Rev. B **30**, 7320 (1984).

Vita

Izabela Anna Szlufarska was born in Wrocław, Poland on March 31, 1975. She went to the XIV High School in Wrocław to a class with an extended program in mathematics, physics and computer science.

After graduating in 1994, she studied at the Wrocław University of Technology, in the Faculty of Basic Problems of Technology with a specialty in Condensed Matter Physics. In 1997, 1998, and 1999 she was awarded Scholarships of the Polish Ministry of National Education. In 1998 she was invited to visit the Center for Theoretical Physics of the Polish Academy of Science in Warsaw and the High Pressure Research Institute for training on crystal growth. In 1999 she visited the University of Tennessee (UT), where she worked with Prof. John J. Quinn on quantum Hall effect and related phenomena. In 1999 she received the Award of the Department of Physics of Wrocław University of Technology for extraordinary laboratory performance and creative writing. The same year she was awarded the MS degree and won the Arkadiusz Piekara Award of the Polish Physical Society for the best MS thesis in physics.

In August 1999 she joined the Physics Department at UT to continue work under Prof. John J. Quinn, Willis Lincoln Chair of Excellence. In 2000 she won the UT Department of Physics and Astronomy award for the best graduate teaching assistant and in 2002 the Fowler-Marion Outstanding Graduate Student Award.

The author has participated and presented her research at a number of international conferences. She was a participant in two research grants funded by the European Union and the Polish State Committee for Scientific Research (KBN). She is the principal author or coauthor of eight journal articles and one textbook for undergraduate physics.

Ms. Szlufarska received the degree of Doctor of Philosophy with a major in Physics in May 2002.